Department of Public Health

Faculty of Medicine

Graduate School of Medicine and Pharmaceutical Sciences

University of Toyama, Toyama, Japan

Mechanistic study of nonivamide enhancement of hyperthermia-induced apoptosis in U937 cells

Sun Lu

Toyama 2019

Contents

Chapter 3

Chapter 4

Abstract

Hyperthermia is one therapeutic tool for damaging and killing cancer cells, with minimal injury to normal tissues. However, its cytotoxic effects alone are insufficient for quantitative cancer cell death. To overcome this limitation, several studies have explored non-toxic enhancers for hyperthermia-induced cell death. Capsaicin may be applicable as a therapeutic tool against various types of cancer. In the present study, I employed nonivamide, a less-pungent capsaicin analogue, to investigate its possible enhancing effects on hyperthermia-induced apoptosis; moreover, I analyzed its molecular mechanism. Treatment of U937 cells at 44°C for 15 min, combined with nonivamide 50 μM, revealed enhancement of apoptosis. Significant increases in reactive oxygen species generation, mitochondrial dysfunction, and cleaved caspase-3 were observed during the combined treatment; these were accompanied by an increase in pro-apoptotic Bcl-2 family proteins and a decrease in anti-apoptotic Bcl-2 proteins. In addition, significant increases in p-JNK and p-p38 were detected, following the combined treatment. In conclusion, nonivamide enhanced hyperthermia-induced apoptosis via a mitochondrial-caspase dependent pathway. The underlying mechanism may include elevation of intracellular reactive oxygen species, mitochondrial dysfunction, and increased activation of JNK and p38.

Keywords

Nonivamide, Hyperthermia, Reactive oxygen species generation, Mitochondrial dysfunction.

Abbreviations

HT, Hyperthermia

Noni, nonivamide

ROS, reactive oxygen species

TRPV1, transient receptor potential cation channel, subfamily V, member 1

NAC, N-acetyl-cysteine

BCH, trans-tert-butylcyclohexanol

DHE, dihydroethidium

TMRM, tetramethylrhodamine methyl ester perchlorate

JNK-IN-8, JNK inhibitor VIII

HSPs, heat shock proteins

MAPKAPK, mitogen-activated protein kinase-activated protein kinases

SHU, Scoville heat units

HO-1, heme oxygenase-1

ER, endoplasmic reticulum

MCU, mitochondrial calcium uniporter

BiP, binding immunoglobulin protein

UPR, unfolded protein response

Chapter 1

Introduction

Hyperthermia, utilized for decades as a useful tumor therapy, induces cell death and activates the immune system [1]. Hyperthermia (up to 44°C) can damage cancer cells with minimal simultaneous injury to normal tissues [2]. When the temperature is above threshold, malignant cells are killed in a time- and temperature-dependent manner [3]. Nevertheless, hyperthermia alone causes insufficient shrinkage of tumors; moreover, nausea, vomiting, and diarrhea are associated with high body temperatures. To overcome these limitations, several studies have explored non-toxic enhancers for hyperthermia-induced cell death [3][4].

Apoptosis, also a type of programmed cell death, is a vital process in all metazoan animals. Ischemic injury, neurodegenerative disorders, and AIDS are all associated with excessive apoptosis [5]. Conversely, promotion of carcinogenesis and progression of tumors are both caused by defective apoptosis [6]. Apoptosis is an important mechanism of hyperthermia-induced cell death [7]. ROS generation is an upstream regulator of the mitochondria-mediated apoptosis pathway, which controls cell proliferation and cell death, cell migration, mitochondrial calcium loading, and other cellular functions [8][9]. In addition to causing other forms of cell death (e.g., necrosis, autophagy, and mitotic catastrophe), conventional chemotherapeutic agents cause significant apoptosis [10]; thus, a great deal of preclinical drug development focuses on regulation of apoptotic signaling.

Nonivamide is a less pungent analogue of capsaicin, which differs from capsaicin by means of one methyl group on the carbon chain and one double bond (Fig. 1A) [11]. Nonivamide-containing cream is used for temporary relief of arthritis and muscle pain in clinical settings. In addition, nonivamide causes multiple physiological effects, including reduced lipid accumulation in pre-adipocyte cells [12], decreased free fatty acid uptake in Caco-2 cells [13], attenuated inflammatory properties in peripheral blood mononuclear

cells [14], and increased dopamine and serotonin release in SH-SY5Y cells [11]. Although capsaicin is reported to have anti-cancer effects [15], the effects of nonivamide on tumor cells remain largely unknown.

A TP53 (Tumor protein p53) gene mutation has been found in more than half of human cancers, suggesting that the TP53 gene plays a crucial role in suppressing tumor formation [16]. Capsaicin can reactivate mutant p53 in glioblastoma and lung cancer [17]; however, leukemic cells with mutant p53 are insensitive to capsaicin [18]. To resolve this incongruity, I have employed hyperthermia and nonivamide, which is a heat-stable analogue of capsaicin (http://www.hmdb.ca/metabolites/HMDB29846), to examine the anti-tumor effects of capsaicin analogues in U937 cells, which are a leukemic cell type with mutant p53 (46 base pair deletions, beginning at codon 132) [14].

This is the first study to reveal that nonivamide, combined with hyperthermia, dramatically suppresses the growth of leukemic cells through the induction of apoptosis. Importantly, I have characterized the molecular mechanisms of nonivamide-enhanced hyperthermia-induced apoptosis in U937 cells.

This thesis is based on the published article. Mechanistic study of nonivamide enhancement of hyperthermia-induced apoptosis in U937 cells, which has been published in "Free Radical Biology and Medicine" [19].

Chapter 2

Materials and Methods

2.1 Reagents

Nonivamide was purchased from Enzo Life Sciences (Farmingdale, NY, USA); capsaicin, AMG 9810, N-acetyl-cysteine (NAC), JNK inhibitor VIII, SB203580, and trans-tert-butylcyclohexanol (BCH) were purchased from Sigma-Aldrich (St. Louis, MO, USA).

2.2 Cell cultures and treatment

Human monocytic leukemia U937 cells were obtained from the Human Sciences Research Resources Bank (Japan Human Sciences Foundation, Tokyo, Japan) and maintained in RPMI-1640 medium, containing 10% inactivated fetal bovine serum (FBS), at 37°C in humidified air with 5% CO_2. For hyperthermia treatment, U937 cells were seeded in plastic tubes at 2.5×10^6 cells/sample, and tubes containing 4 mL of suspension cell culture, immersed in a precision-controlled water bath, were incubated at 37°C or 44°C for 3 h. Indicated concentrations of nonivamide were added to the medium 30 min before heating. HeLa, HepG2, and HEK293 cells were obtained from the Japan Cancer Research Resources Bank (Tokyo, Japan). The HaCaT cell line was a generous gift from Dr. Ogawa (Department of Radiological Sciences; University of Toyama). HeLa, HepG2, HEK293, and HaCaT cells were grown in Dulbecco's Modified Eagle's Medium (DMEM), containing 10% heat-inactivated fetal bovine serum (FBS), and maintained in a humidified incubator at 37°C with 5% CO_2. For hyperthermia treatment, cells were seeded at 2×10^5 cells/plate in 35mm plates, then incubated at 37°C or 44°C for 30 min, using a precision-controlled water bath. Indicated concentrations of nonivamide were added to the medium 30 min before heating and the cells were incubated for an additional 24 h following hyperthermia treatment.

2.3 Cell proliferation assay

Cell viability was determined by the Cell Counting Kit-8 (CCK-8) (Dojindo Lab., Kumamoto, Japan). After U937 cells were exposed to heat shock at 44°C for 15 min with or without nonivamide, they were seeded in 96-well plates at 5×10^3 cells/well and incubated for 24, 48, or 72 h at 37°C in 5% CO_2, then incubated for an additional 2 h with 10 μL CCK-8 solution, under the same environmental conditions. Cell absorbance at 450 nm was measured by a uQuant Universal Microplate Spectrophotometer (Bio-Tek Instruments, Winooski, VT, USA).

2.4 Detection of apoptosis with flow cytometry and Hoechst 33258

Cells were stained with Annexin V-fluorescein isothiocyanate (FITC) and propidium iodide, then were analyzed by flow cytometry (EPICS XL, Beckman-Coulter, Miami, FL, USA), according to the manufacturer's protocol [20].

After collection, cells were fixed with 4% paraformaldehyde in phosphate-buffered saline (PBS) for 30 min at 4°C, then stained with 1 mM Hoechst 33258 for 5 min. Shrunken cell bodies, nuclear fragmentation, and formation of apoptotic bodies were detected using a fluorescence microscope (BX-61, Olympus, Tokyo, Japan) with a 20× objective lens. Analysis of apoptosis by propidium iodide staining and flow cytometry was performed as in a previous protocol [21].

2.5 Assessment of DNA fragmentation

A quantitative DNA fragmentation assay was performed according to the method of Sellins and Cohen, with a few modifications [22]. After incubation for 3 h, cells were harvested and lysed in a lysis buffer (10 mM Tris, 1 mM EDTA, 0.1% NP-40; pH 7.5). After centrifugation at 13,000 ×g for 10 min to separate intact and fragmented chromatin (DNA), both types of DNA were separately precipitated, overnight at 4°C in 12.5% trichloroacetic acid (TCA). After hydrolysis in 5% TCA at 90°C for 20 min, each type (intact/fragmented) of DNA precipitate was quantified. Absorbance at 600 nm was measured after overnight color development (DU-50, Beckman-Coulter), using a diphenylamine (DPA) reagent. ‘‘Percent fragmentation’’ refers to the ratio of DNA in the fragmented chromatin to the total DNA (fragmented + intact).

2.6 Intracellular reactive oxygen species

Using flow cytometry, intracellular ROS levels were detected using dihydroethidium (HE; Molecular Probes, Eugene, OR, USA). HE exhibits blue fluorescence in the cytosol until oxidized by superoxide to 2-hydroxyethidium, which then intercalates within cellular DNA, staining the nucleus a bright fluorescent red. After incubation with 4 μM HE for 15 min at 37°C, cells were washed twice with PBS; the percentage of intracellular ROS was estimated by flow cytometry.

2.7 Mitochondrial membrane potentials

After 2h incubation in hyperthermic conditions, with or without nonivamide, cells were collected and treated with 10 nM tetramethylrhodamine methyl ester perchlorate (TMRM) (Molecular Probes, Eugene, OR, USA), in 1 mL of 1% fetal bovine serum in

PBS, for 15 min at 37°C. As TMRM is a cationic fluorophore, which is widely used for staining cellular mitochondria and the mitochondrial matrix, the percentage of cells with mitochondrial membrane potential (MMP) loss was analyzed by flow cytometry gated on red TMRM fluorescence (excitation at 488 nm; emission at 575 nm) .

2.8 Calcium

Intracellular Ca^{2+} flux was monitored with flow cytometry, using Rhod-2/AM and Fluo-3/AM (Molecular Probes). Labeled calcium indicators exhibited an increase in fluorescence upon binding to Ca^{2+}. After routine treatment, U937 cells were loaded with cell-permeant calcium indicators, 4 μM Rhod-2/AM or Fluo-3/AM, in Hank's balanced salt solution (HBSS) for 30 min at 37°C. The fluorescence intensity was measured by flow cytometry (Rhod-2/AM excitation at 550 nm, emission at 575 nm; Fluo-3/AM excitation at 488 nm, emission at 526 nm).

2.9 Western blot analyses

After harvest and washing with PBS, cells were lysed in a RIPA buffer (150 mM NaCl, 1% Triton X-100 (v/v), 1% sodium deoxycholate, 0.1% SDS, 1 μg/mL each of aprotinin, pepstatin, and leupeptin, 1 mM EGTA, 50 mM Tris–HCI, pH 7.5) for 20 min on ice. After a brief sonication, lysates were centrifuged at 13,000 ×g for 10 min at 4°C. Cell lysates were electrophoresed on 10% SDS-PAGE and then transferred to PVDF membranes. Each membrane was blocked with 5% skim milk in Tris-buffered saline with Tween (TBST; 150 mM NaCl, 50 mM Tris, pH 7.5, 0.1% Tween-20). Western blot analyses of Mcl-1, XIAP, cleaved caspase-3, JNK, phospho-JNK (p-JNK), ERK1/2,

phospho-ERK1/2 (p-ERK), p38, phospho-p38 (p-p38), HSP27, phospho-HSP27 (p-HSP27), phospho-PKCδ Thr505 (p-PKCδ), PKCδ, AKT (pan), phospho-AKT Ser473 (p-AKT), phospho-GSK-3 beta Ser9 (p-GSK), GSK-3 beta (Cell Signaling Technology, Inc., Beverly, MA, USA), Bcl-2, Bcl-xL, Bax, Bid, and beta-actin (Santa Cruz Biotechnology, Inc., Santa Cruz, CA) were performed using specific monoclonal or polyclonal antibodies. For detection, the chemiluminescence agent ECL was used according to manufacturer's instructions (Amersham Biosciences, Buckinghamshire, UK) [23]. All images were quantified using ImageJ software (National Institute of Mental Health, Bethesda, MA, USA).

2.10 Statistics

All experiments were three biological replicates of independent experiments. Data are expressed as mean ± standard deviation (SD). Multiple comparisons were performed using analysis of variance (ANOVA) followed by one-way ANOVA, or using two-way ANOVA with Dunnett's test. $P < 0.05$ was considered to be statistically significant.

Chapter 3

Results

3.1 Combined treatment of nonivamide with hyperthermia markedly enhanced apoptosis and cytotoxicity in U937 cells

Previously, some compounds (e.g., DHA and withaferin A) were found to significantly enhance hyperthermia-induced apoptosis in U937 cells [24,25]. By fluorescent microscopy, I found hyperthermia combined with nonivamide induced more morphological changes in the nuclei (typically observed in apoptosis) than were induced by hyperthermia alone (Fig. 1B). Flow cytometry analysis indicated similar changes. Hyperthermia (44°C, 15 min) alone induced moderate apoptosis in U937 cells (23.43±1.6%; Fig. 1C), after 3 h of incubation; notably, hyperthermia combined with nonivamide promoted apoptosis in a dose-dependent manner (Fig. 1D), inducing cell apoptosis in 42.9±1.7% of cells that were treated with hyperthermia and nonivamide 50 μM (Fig. 1E). However, treatment with nonivamide 50 μM alone did not induce apoptosis in U937 cells, as demonstrated by DNA fragmentation and Hoechst staining (Supplement Fig. 1A and B). *In vitro*, the uptake efficiency of spice principles in rat peritoneal macrophages exhibited an inverse relationship with the concentration of the spice principle. For example, the uptake efficiency of capsaicin was 76%–82% at concentrations of 5–10 μM, whereas the uptake efficiency of curcumin was 89% at 50 μM [26]. Based on these data and another previous report [14], nonivamide 50 μM was selected as the maximum concentration in this study.

The CCK-8 assay was employed to detect cell viability, nonivamide 50 μM combined with hyperthermia was found to suppress cell proliferation more than hyperthermia alone. Moreover, after 72 h, cells regained proliferative ability only in the group that received hyperthermia treatment, but not in the group that received combination treatment (Fig.

1F), indicating that nonivamide could enhance hyperthermia-induced suppression of cancer cell proliferation.

To confirm this effect, I introduced two other adherent cancer cell lines, HepG2 and HeLa. I detected apoptosis using flow cytometry via PI staining, where the sub G1 population indicated apoptosis ratio. In these experiments, the hyperthermia plus nonivamide group exhibited a significant increase in sub G1 population, compared with hyperthermia alone (Fig. 1G, H). Thus, hyperthermia combined with nonivamide treatment was effective against U937 cells and against other cancer cell lines. Previous studies have demonstrated that animal exposure to 50°C causes virtually no injury to normal tissues [2,27]. To determine the effect of hyperthermia plus nonivamide on non-cancerous cells, I studied human immortalized embryonic kidney (HEK293) cells and immortalized keratinocytes (HaCaT cells). I found no statistical difference between groups treated with hyperthermia and hyperthermia combined with nonivamide (Fig. 1I, J). Therefore, compared with hyperthermia alone, hyperthermia combined with nonivamide 50 μM did not enhance obvious apoptosis in non-cancerous cells.

3.2 Hyperthermia combined with nonivamide increased reactive oxygen species generation

Hyperthermia has been reported to increase ROS generation, thereby disturbing the mitochondrial membrane and impacting cellular apoptosis [7]. Therefore, as a next step, I examined intracellular ROS generation by means of flow cytometry (Fig. 2A). From time course experiments, I determined the optimal time point for comparing ROS generation (Supplement Fig. 3A). Combined treatment with nonivamide 50 μM significantly up-regulated ROS generation (51.6±3.1%), compared with hyperthermia

alone (22.2±4.7%). Combined treatment of nonivamide with hyperthermia promoted ROS production in a concentration-dependent manner (Fig. 2B). Next, I employed NAC (a precursor of the endogenous antioxidant glutathione), which was reported to protect against X-ray- or hyperthermia-induced apoptosis in U937 cells [28], to examine whether ROS generation was involved in the induction of apoptosis. Pre-incubation with NAC (2.5 mM, 30 min) attenuated the combined treatment enhancement of ROS generation (28.1±5.0%) (Fig. 2B). These results indicated that enhancement of nonivamide-induced apoptosis was mediated by intracellular ROS generation.

3.3 Combined treatment of nonivamide with hyperthermia evoked mitochondrial dysfunction

Hyperthermia has been shown to cause mitochondrial dysfunction [7]. In our current study, cells exposed to combined treatment (hyperthermia and nonivamide) exhibited enhanced MMP reduction, in a dose-dependent manner (Fig. 3A). MMP was reduced by up to 21.5±4.4% in cells treated with hyperthermia (44°C, 15 min) and nonivamide 50 μM. In contrast, U937 cells exposed to hyperthermia alone did not exhibit obvious mitochondria dysfunction (Fig. 3B).

Oxidative stress promoted mitochondrial calcium overloading and mitochondrial permeability transition pore opening, then led to pro-apoptotic protein release from mitochondria into the cytosol, triggering intrinsic pathways of apoptosis [29]. Because the combined treatment caused upregulation of ROS generation and led to disrupted MMP, I examined whether combined treatment could result in changes in mitochondrial Ca^{2+} flux. As shown in Fig. 3C, nonivamide 50 μM combined with hyperthermia

significantly increased mitochondrial Ca^{2+} loading; this trend could be abrogated by the ROS scavenger NAC (Fig. 3D). These results indicated that ROS generation may play a key role in the above processes, and the hyperthermia plus nonivamide could enhance the mitochondria-mediated apoptotic pathway in U937 cells.

3.4 Changes in expression of anti- and pro-apoptotic proteins

Expression of anti- and pro-apoptotic members of the Bcl-2 family forms a delicate balance, which tightly regulates MMP loss and apoptosis [6]. Hyperthermia with or without nonivamide treatment did not affect XIAP and Bax expression. The expression of pro-survival Bcl-2 proteins—Bcl-2, Bcl-xL, and Mcl-1—decreased dramatically (Fig. 4A, B). In contrast, expression of pro-apoptotic Bcl-2 family proteins, including truncated Bid (tBid) and the hallmark apoptotic protein, cleaved caspase 3, was up-regulated (Fig. 4C, D). These results suggest that treatment with nonivamide combined with hyperthermia disturbs the balance of anti-apoptotic and pro-apoptotic proteins. In contrast, hyperthermia alone did not dramatically impact the expression of pro- or anti-apoptotic members of the Bcl-2 family.

The PKC family plays an important role in oxidative stress and DNA damaging agent-induced apoptosis [30]. In particular, PKCδ plays a critical role in the pro-apoptotic signaling pathway; cleaved caspase-3 activates proteolytic cleavage of PKCδ in response to apoptotic signals in U937 cells [31]. Previously, I reported that DHA combined with hyperthermia was capable of increasing ROS generation [32]; this oxidative stress subsequently induced PKCδ phosphorylation and cleavage. Thus, I examined the expression level of PKCδ. Combined treatment of hyperthermia with nonivamide

significantly up-regulated the cleaved fragment expression level of p-PKCδ, an active form of PKCδ, compared with hyperthermia alone (Fig. 4C). Hence, nonivamide augmented the effect of hyperthermia-induced apoptosis on a mitochondria-dependent pathway; the activation fragment of p-PKCδ may also be involved in this pathway.

3.5 Modulation of MAPK and AKT signal-transduction pathway-associated proteins

Next, I investigated which signaling pathway mediated the enhanced effect of nonivamide on hyperthermia-induced apoptosis. First, to investigate the possible role of MAPK pathways in the nonivamide-enhanced apoptotic effect, phospho-JNK (p-JNK), phospho-p38 (p-p38), and phospho-ERK (p-ERK) were examined by western blot analysis. Neither combined nor individual treatments changed the expression of total JNK, p38, or ERK1/2 (Fig. 5A and C). After 20 min incubation, hyperthermia alone increased p-JNK and p-p38 expression. More significant upregulation was observed during combined treatment (Fig. 5A). Unexpectedly, hyperthermia alone rapidly changed the expression of p-ERK, whereas the combined treatment did not change its expression. There was not a significant difference between individual treatment and combined treatment in the expression of p-ERK (Fig. 5A). By prolonging the incubation time from 20 min to 1 h, the p-JNK and p-p38 expression gradually increased for both conditions. The nonivamide 50 μM combined group significantly up-regulated p-JNK and p-p38 expression, compared with hyperthermia alone, following 1 h incubation (Fig. 5C). To determine whether p-JNK and p38 were involved in this process, I utilized JNK inhibitor VIII and SB203580 (a p38 inhibitor). As expected, the JNK inhibitor abolished nonivamide combined treatment-enhanced apoptosis by inhibiting p-JNK expression

(Fig. 6B and E), whereas SB203580 rescued nonivamide plus hyperthermia-induced apoptosis by blocking p-p38 expression (Supplemental Fig. 4C–F). Moreover, NAC could partially rescue nonivamide combined treatment-induced apoptosis, via inhibition of p-JNK expression (Fig. 6B and E). These results suggested that JNK, activated by ROS generation, may be involved in the enhanced apoptosis caused by the combined treatment.

Phosphatidylinositol 3-kinase (PI3K) and Protein Kinase B (AKT) pathways play a critical role in cell proliferation and survival [33]. Thus, I next examined the changes to these pathways. Nonivamide combined with hyperthermia induced apoptosis, which disrupted cell survival and dramatically decreased the expression of phospho-AKT (p-AKT) (Fig. 5E). Activity of GSK-3 beta, a critical downstream element of the PI3K/AKT pathway, could be inhibited by p-AKT mediated phosphorylation at Ser9. p-GSK-3 beta demonstrated a similar trend to p-AKT (Fig. 5E). Hence, p-AKT and p-GSK-3 beta expression was attenuated in a time-dependent manner. However, following 1 h incubation, hyperthermia alone caused obvious suppression of p-AKT and p-GSK-3 beta expression, whereas the combined treatment did not. Thus, the PI3K/AKT/GSK-3 beta pathway was involved in hyperthermia-induced apoptosis; nonivamide combined with hyperthermia treatment did not exert a synergistic effect in suppressing p-AKT and p-GSK-3 beta expression (Fig. 5G).

3.6 BCH partially rescued nonivamide enhancement of hyperthermia treatment-induced apoptosis

As a capsaicin analogue, nonivamide has been reported to activate the TRPV1 channel [14]. A previous study revealed that nonivamide exhibited anti-inflammatory effects in U937 cells via the TRPV1 channel, and that this anti-inflammatory effect was inhibited by the TRPV1 antagonist, tert-butylcyclohexanol (BCH) [14]. Therefore, I used BCH to examine whether TRPV1 was involved in the enhancing effect of nonivamide on hyperthermia-induced apoptosis. U937 cells were pre-treated with BCH for 30 min; then, 30 min prior to hyperthermia, nonivamide 50 μM was added. The individual or combined treatment could not dramatically increase intracellular calcium (Supplement Fig. 4). Moreover, BCH could not decrease the enhanced ROS generation following hyperthermia combined with nonivamide treatment (data not shown), nor did it affect mitochondrial calcium overloading (Fig. 3D). Western blotting indicated that BCH partially blocked the up-regulated expression of p-JNK1 that resulted from nonivamide combined treatment (Fig. 6C, D). Therefore, BCH appears to attenuate nonivamide combined treatment-induced apoptosis via the JNK pathway (Fig. 6A, C). Similar results were achieved using another antagonist, AMG 9810 (Fig. 6A). TRPV1 antagonists, in addition to blocking the TRPV1 channel, exhibited different biological activities. BCH could not enhance hyperthermia-induced apoptosis, whereas capsazepine, a widely used TRPV1 antagonist, significantly promoted hyperthermia-induced programmed cell death (Supplement Fig. 1D). Taken together, these data suggest that the enhancing effect of nonivamide on hyperthermia-induced apoptosis may be independent of the TRPV1 channel.

Figures

Fig. 1A

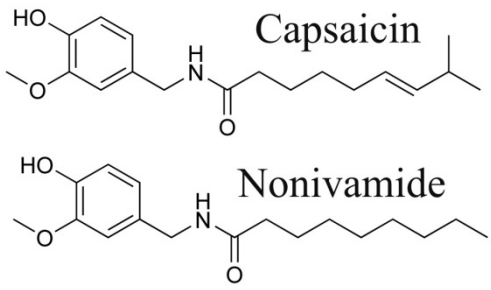

Fig. 1B

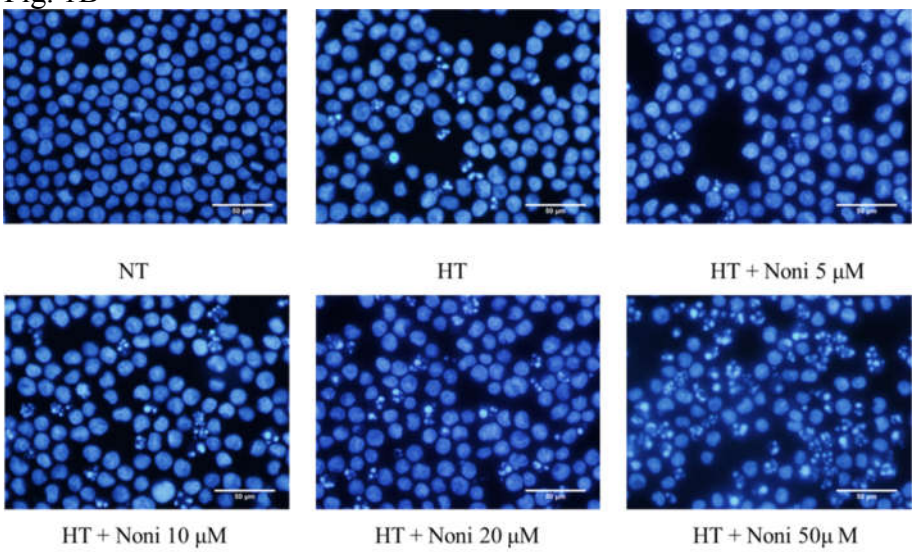

Fig. 1C

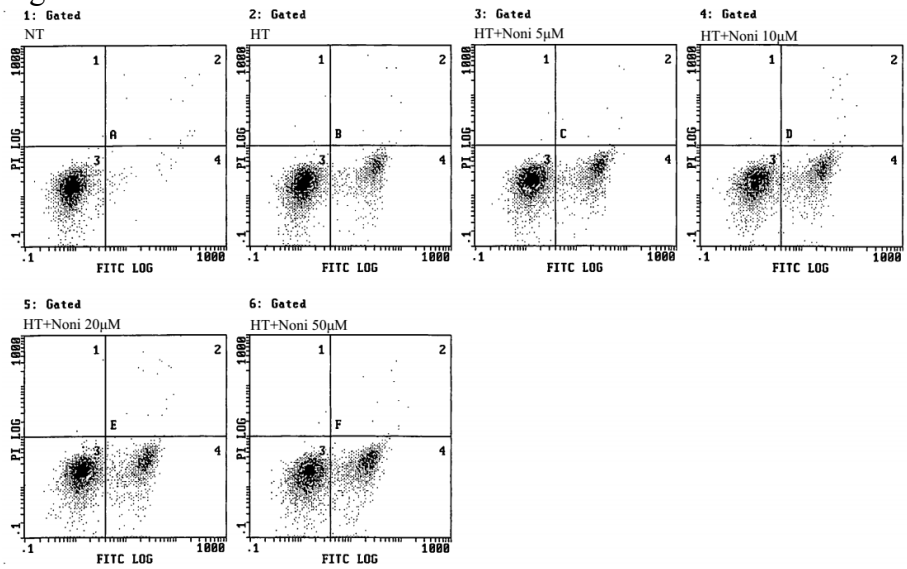

Fig. 1D

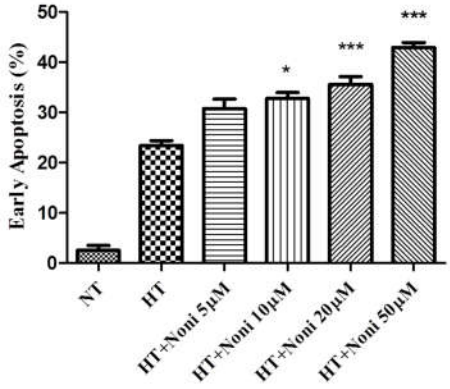

Fig. 1E

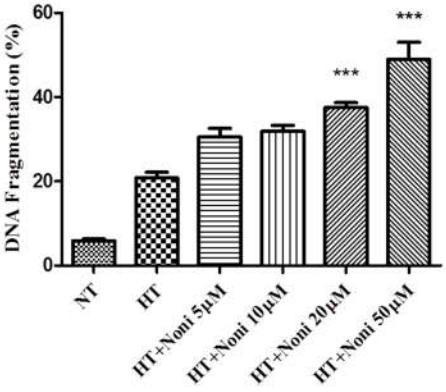

Fig. 1F

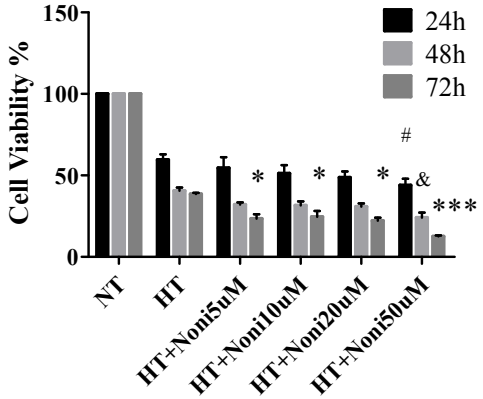

Fig. 1G

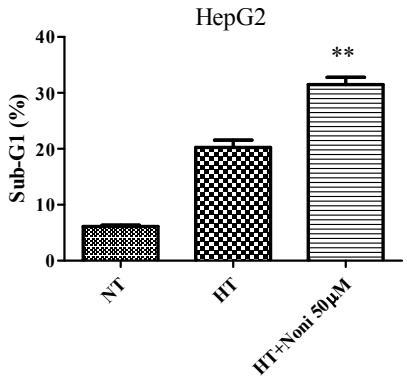

Fig. 1H

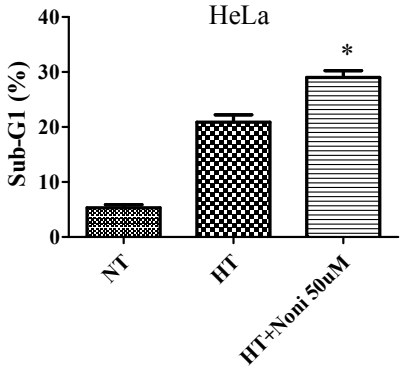

Fig. 1I

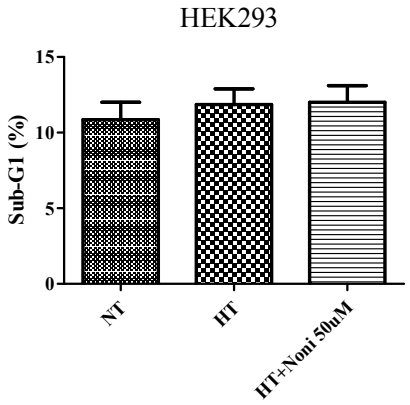

Fig. 1J

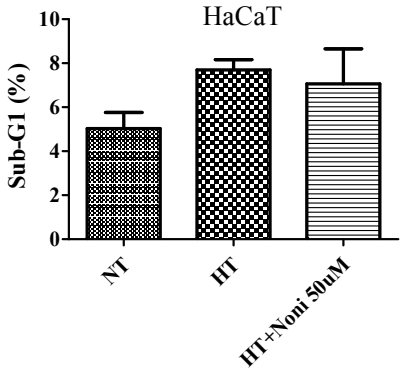

Figure 1: Combined treatment of nonivamide with hyperthermia markedly enhanced apoptosis and cytotoxicity in U937 cells.

The chemical structures of capsaicin and nonivamide (A). U937 cells were treated with hyperthermia for 15 min at 44°C, with or without pre-treatment with nonivamide, followed by 3 h incubation. The morphological changes of nuclei were determined by Hoechst staining (B). Apoptosis was evaluated using flow cytometry with annexin V/FITC and PI dual staining (C, D). DNA fragmentation rate was determined by DNA fragmentation assay (E). Cell viability was evaluated by using Cell Counting Kit 8 (F). HepG2 (G), HeLa (H), HEK293 (I), and HaCaT (J) cells were treated with hyperthermia for 30 min at 44°C, with or without pre-treatment with nonivamide, followed by 24 h incubation. Apoptosis was analyzed by propidium iodide staining and flow cytometry. The data are expressed as mean ± SEM from three independent experiments. Statistical analysis in D, E, G–J was performed using one-way ANOVA (Dunnett's test), in which $*p < 0.05$ and $***p < 0.001$ versus the hyperthermia group. Statistical analysis in F was performed using two-way ANOVA, in which #, and $*p < 0.05$ versus the hyperthermia group at 24, 48, and 72 h.

Fig. 2A

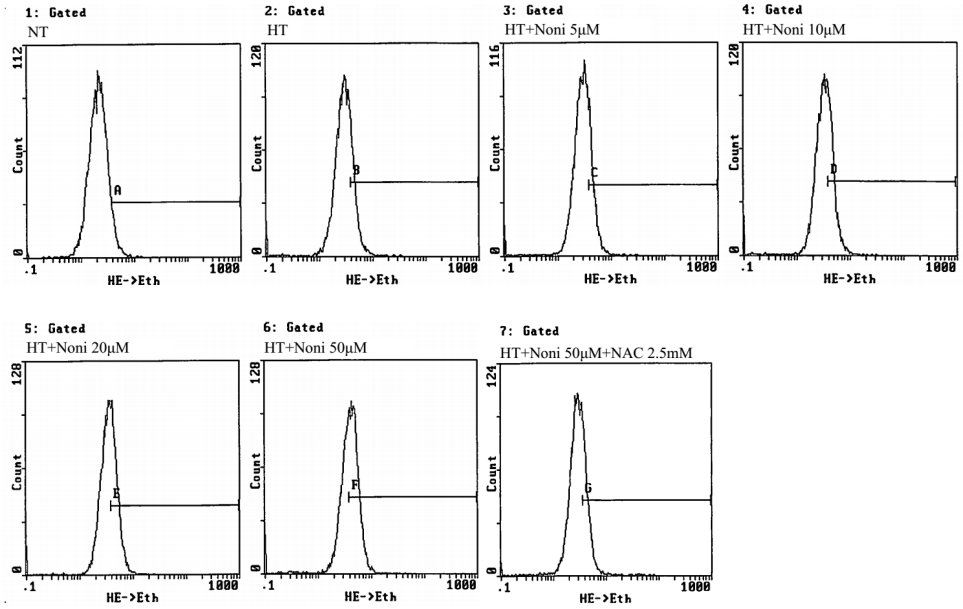

Fig. 2B

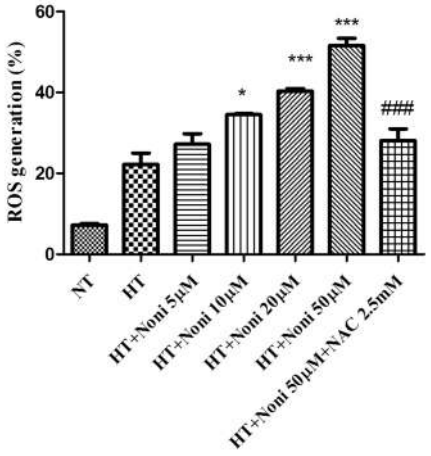

Figure 2: Combined treatment of nonivamide with hyperthermia caused increased reactive oxygen species (ROS) generation.

Intracellular O_2 generation was measured using flow cytometry with HE staining (A, B). The increase in the fraction of cells with higher intensities was measured by comparing with the same fraction of from cells that only experienced hyperthermia. The data are expressed as mean ± SEM from three independent experiments. Statistical analysis was performed by one-way ANOVA (Dunnett's test), in which *$p < 0.05$ & ***$p < 0.001$ versus the hyperthermia group, and ### $p < 0.001$ versus the nonivamide 50 μM combined hyperthermia group.

Fig. 3A

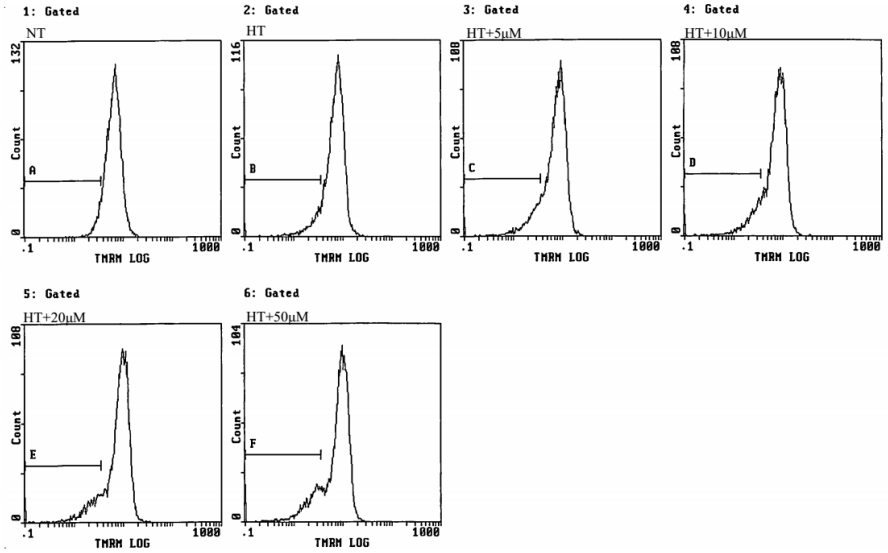

Fig. 3B

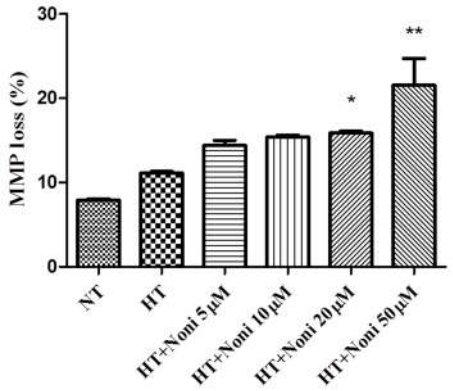

Fig. 3C

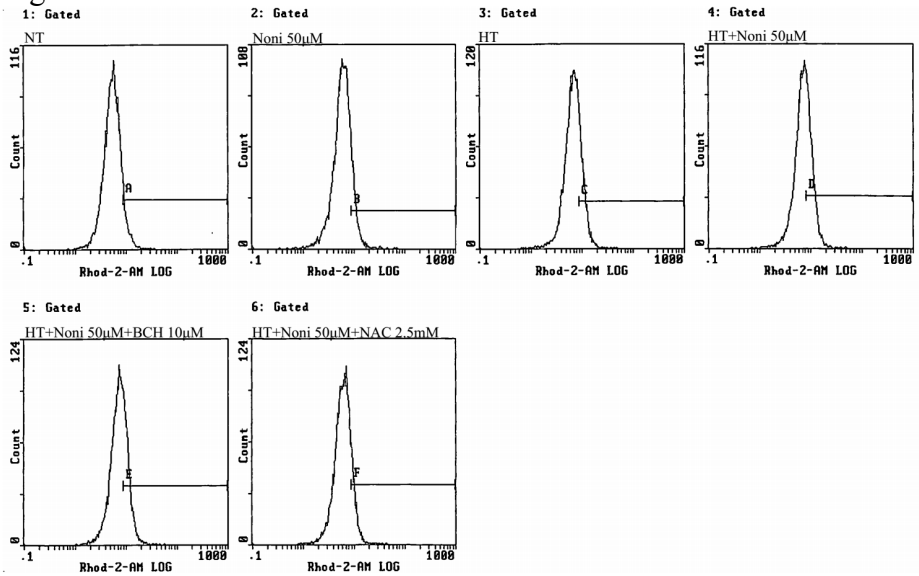

Fig. 3D

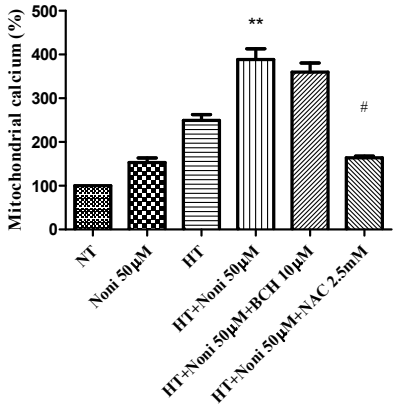

Figure 3: Combined treatment of nonivamide with hyperthermia evoked mitochondrial dysfunction.

Exposure of U937 cells to nonivamide combined hyperthermia with 2 h incubation caused disruption of mitochondrial transmembrane potential (A, B). After routine treatment, cells were loaded with cell-permeant calcium indicators to determine the mitochondrial Ca^{2+}. Nonivamide combined treatment-induced the elevation of mitochondrial Ca^{2+} levels in U937 cells (C, D). The data are expressed as mean ± SEM from three independent experiments. Statistical analysis was performed by one-way ANOVA (Dunnett's test), in which *$p < 0.05$, **$p < 0.01$ versus the hyperthermia group, and # $p < 0.01$ pre-treatment with the NAC group versus the nonivamide 50 μM combined group.

Fig. 4A

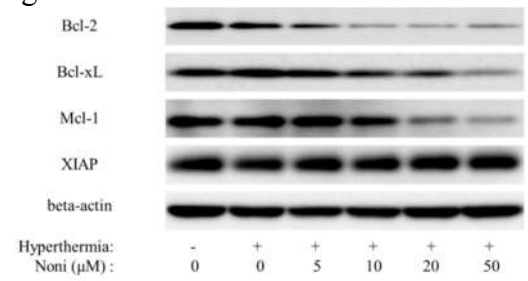

Fig. 4B

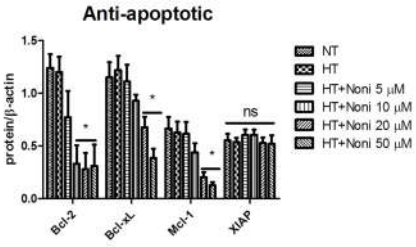

Fig. 4C

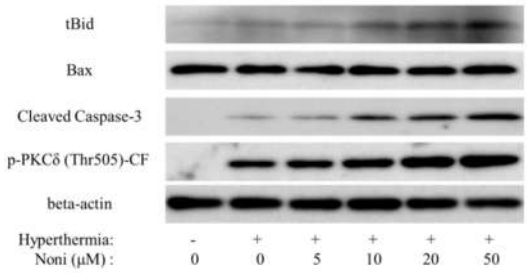

Fig. 4D

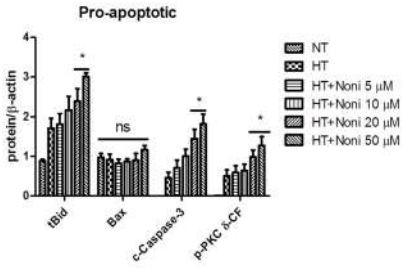

Figure 4: Changes in expression of anti- and pro-apoptotic proteins.

After treatment with or without nonivamide at the indicated concentrations for 3 h, the expression of anti-apoptotic proteins was determined by western blot (A). Anti-apoptotic protein levels, vs. control, were quantified and standardized against beta-actin (B). Expression of pro-apoptotic proteins was analyzed by western blot (C). Pro-apoptotic protein levels, vs. control, were quantified and standardized against beta-actin (D) Representative data are shown from three separate experiments. Statistical analysis was performed by one-way ANOVA (Dunnett's test), in which *$p < 0.05$ versus the hyperthermia group, ns=non-significant.

Fig. 5A

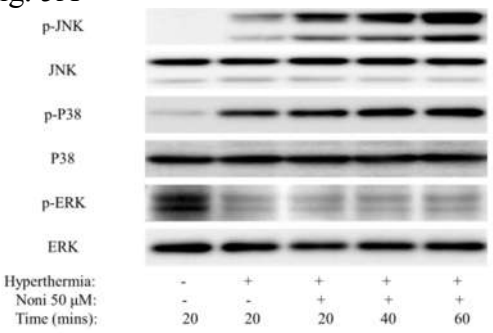

Fig. 5B

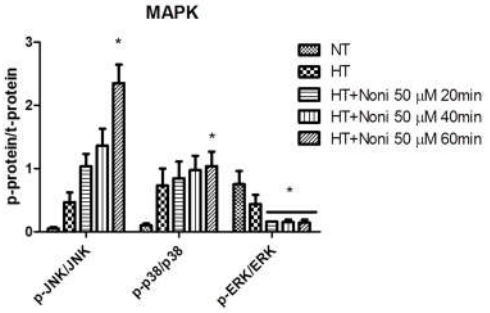

Fig. 5C

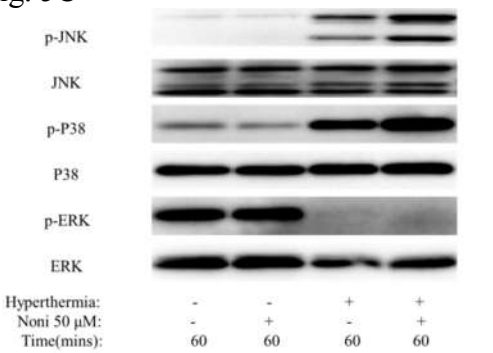

Fig. 5D

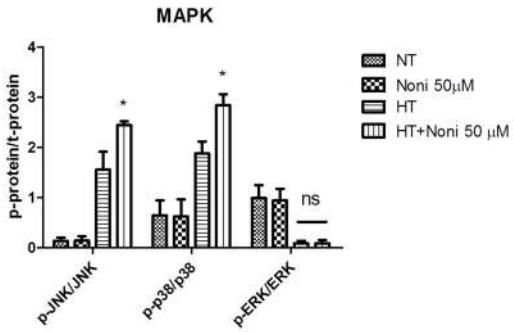

Fig. 5E

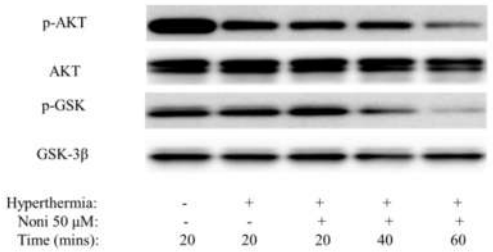

Fig. 5F

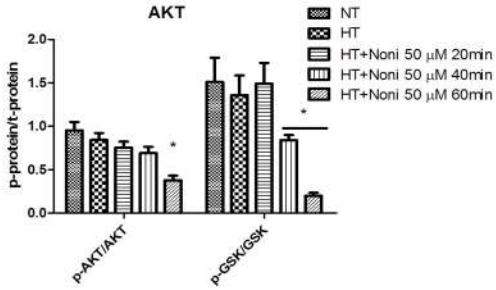

Fig. 5G

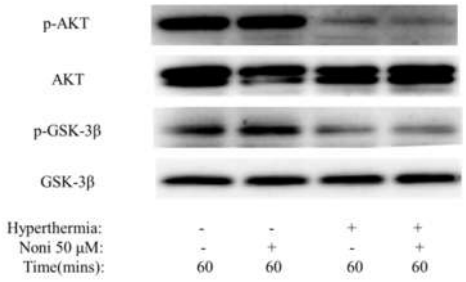

Fig. 5H

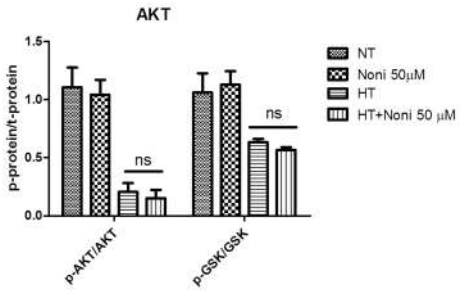

Figure 5: Modulation of MAPK and AKT signal-transduction pathway associated proteins.

U937 cells were exposed to individual and combined treatment and the observed expression of phosphorylated and total forms of JNK, ERK, and p38 was analyzed by

western blot (A, C). Average values of the ratio of phosphorylated to total proteins were quantified in each group (B, D). The expression of phosphorylated and total forms of AKT and GSK-3 beta were analyzed by western blot (E, G). Average values of the ratio of phosphorylated to total proteins were quantified in each group (F, H). Representative data are shown from three separate experiments. Statistical analysis was performed by one-way ANOVA (Dunnett's test), in which *$p < 0.05$ versus the hyperthermia group, ns=non-significant.

Fig. 6A

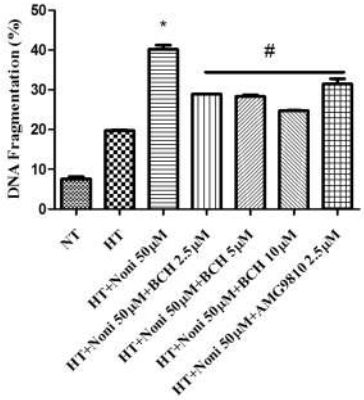

Fig. 6B

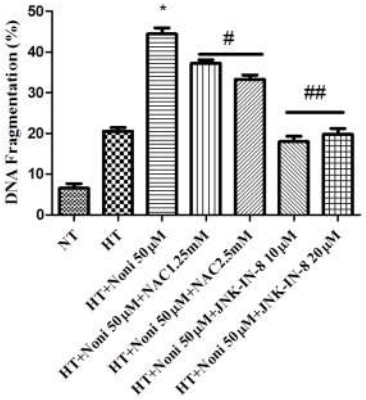

Fig. 6C

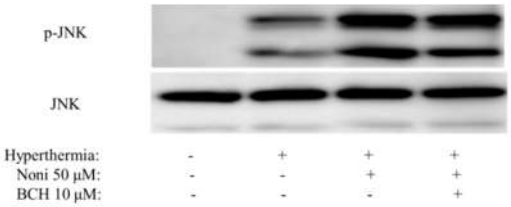

Fig. 6D

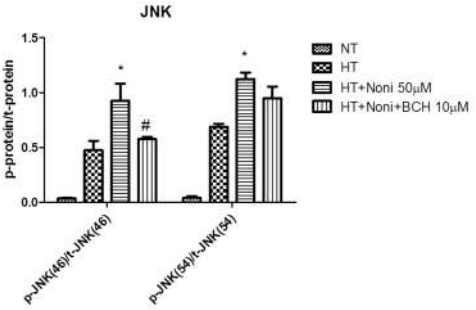

Fig. 6E

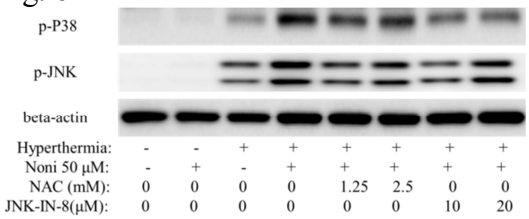

Fig. 6F

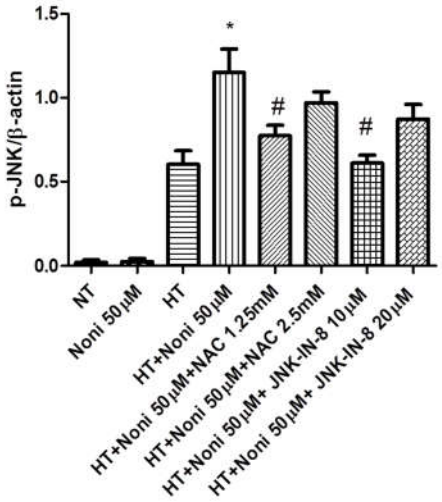

Fig. 6G

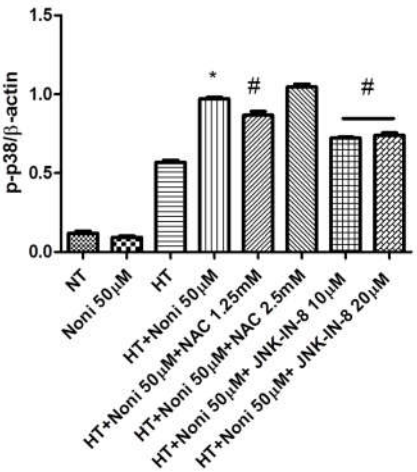

Figure 6: BCH partially rescued nonivamide combined hyperthermia treatment-induced apoptosis.

U937 cells were pre-incubated with NAC, BCH, AMG 9810, or JNK-IN-8 for 30 min, respectively, and DNA fragmentation rate was determined by DNA fragmentation assay (A, B). Expressions of phosphorylated forms of JNK and p38 were analyzed by western blot (C, E). Average values of the ratio of phosphorylated to total proteins (D) or beta-actin (F, G) were quantified in each group. Representative data are shown from three separate experiments. The data are expressed as mean ± SEM from three independent experiments. Statistical analysis was performed by one-way ANOVA (Dunnett's test), in which *$p < 0.01$ versus the hyperthermia group, and # $p < 0.05$ and ##$p< 0.01$ pre-treatment with the inhibitor group versus the nonivamide 50 μM combined group.

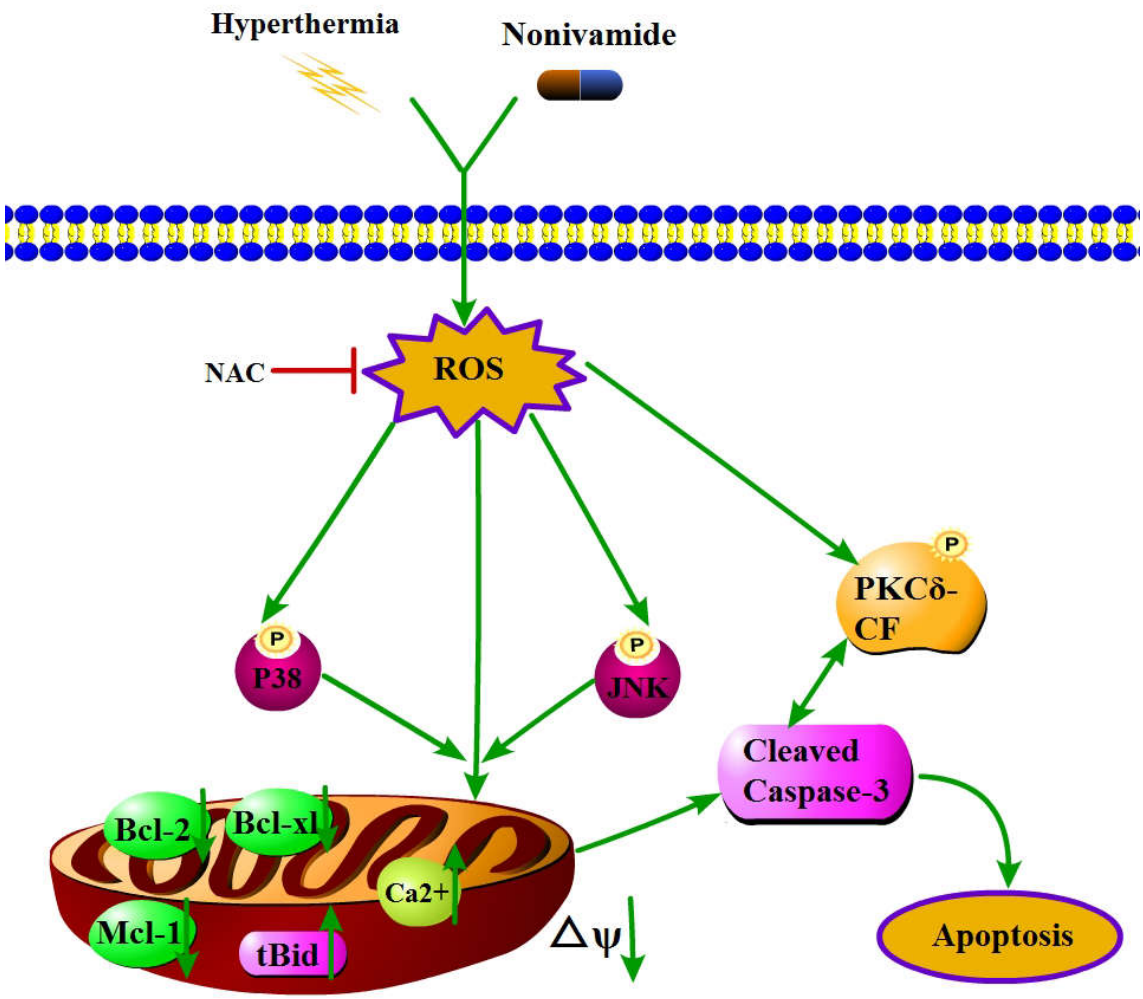

Figure 7: Schematic model for nonivamide-enhanced hyperthermia-induced apoptosis.

Combined hyperthermia with nonivamide treatment induces excessive generation of intracellular ROS; in this oxidative stress condition, p38, JNK, and PKC-delta are phosphorylated. Additionally, the ROS generation causes mitochondria calcium overload, promoting apoptosis. Changes in the ratio of anti- and pro-apoptotic proteins (Bcl-2, Bcl-xL, and Mcl-1; and tBid, respectively) also contribute to apoptosis. ΔΨ: mitochondrial membrane potential.

Supplemental Figure

Supplement Fig. 1A

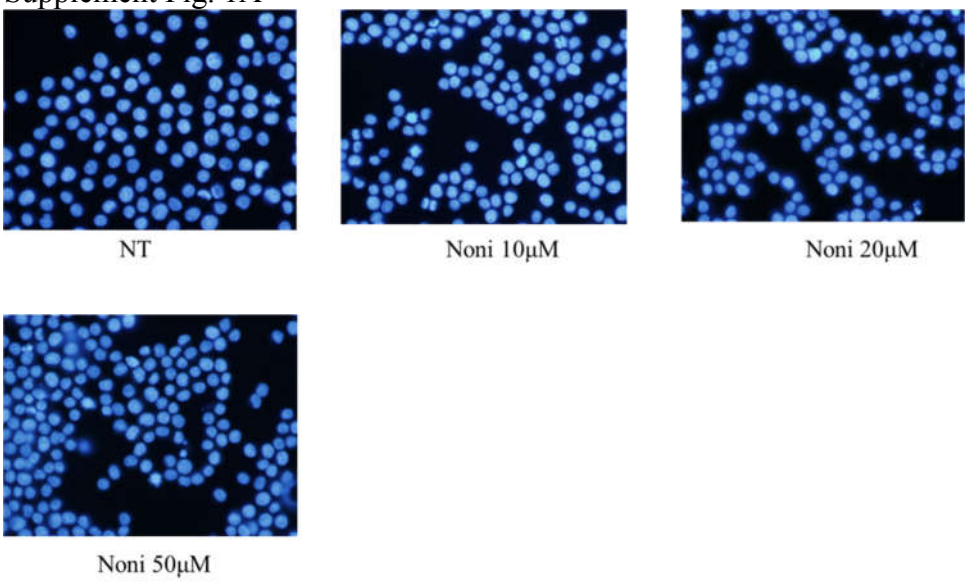

Supplement Fig. 1B

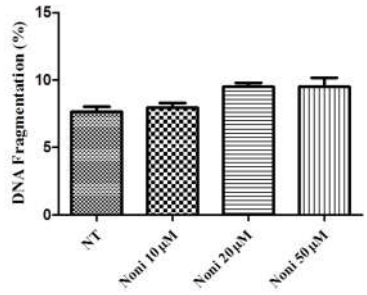

Supplement Fig. 1C

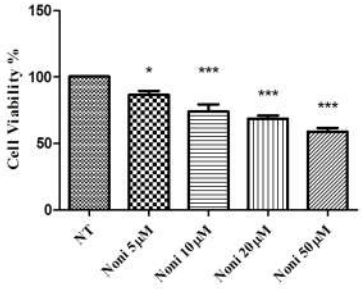

Supplement Fig. 1D

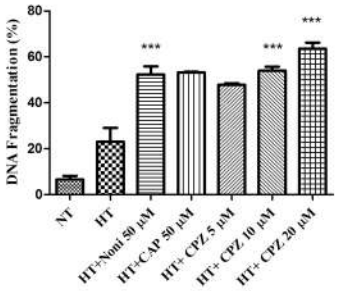

Supplemental Figure 1: Nonivamide alone-induced cytotoxicity and capsaicin or capsazepine combined with hyperthermia-induced apoptosis in U937 cells.

U937 cells were treated with nonivamide followed by 24 h incubation. The morphological changes of nuclei were determined by Hoechst staining (A). Apoptosis was evaluated using the DNA fragmentation rate (B). Cell viability was evaluated by using Cell Counting Kit 8 (C). U937 cells were treated with hyperthermia for 15 min at 44°C, with or without pre-treatment with nonivamide (Noni), capsaicin (CAP), or capsazepine (CPZ), followed by 3 h incubation; apoptosis was evaluated using the DNA fragmentation rate (D). The data are expressed as mean ± SEM from three independent experiments. Statistical analysis was performed by one-way ANOVA (Dunnett's test), in which ***$p < 0.001$ versus the hyperthermia alone group.

Supplement Fig. 2A

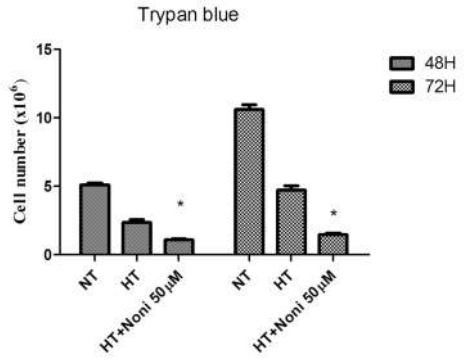

Supplement Fig. 2B

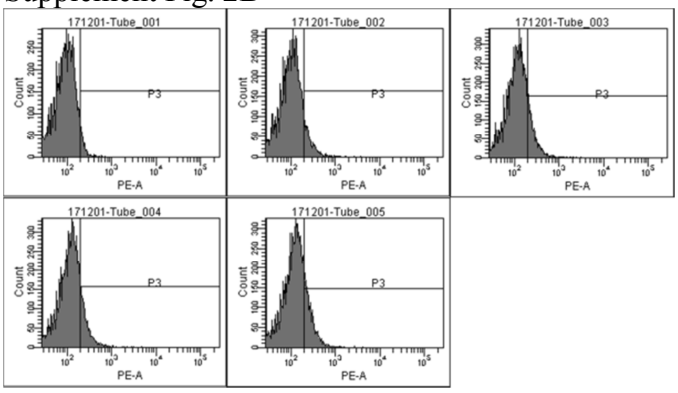

Supplement Fig. 2C

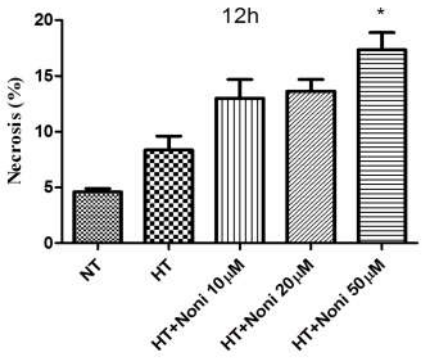

Supplemental Figure 2: Combined treatment of nonivamide with hyperthermia markedly enhanced necrosis and cytotoxicity in U937 cells.

U937 cells were treated with hyperthermia for 15 min at 44°C, with or without pre-treatment with nonivamide. Cell viability was evaluated using the Trypan blue exclusion method (A). Necrosis was evaluated using flow cytometry with PI staining, followed by 12 h incubation (B, C). Statistical analysis was performed by one-way ANOVA (Dunnett's test), in which *$p < 0.05$ and ***$p < 0.01$ versus the hyperthermia group.

Supplement Fig. 3A

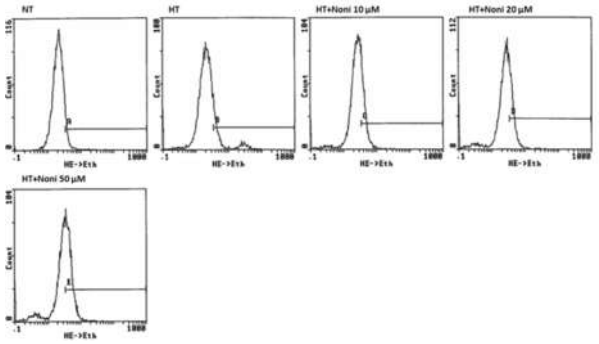

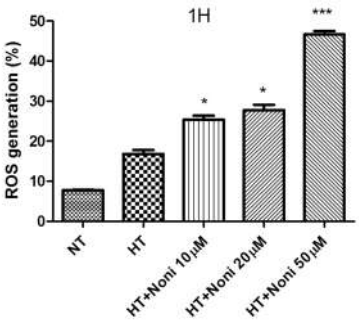

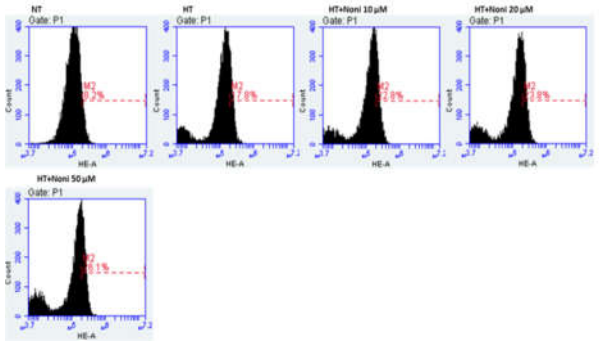

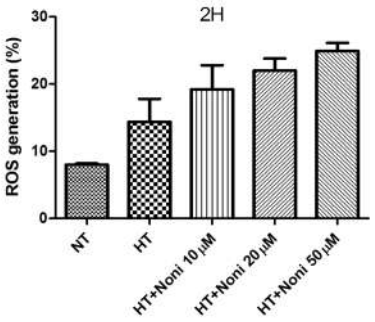

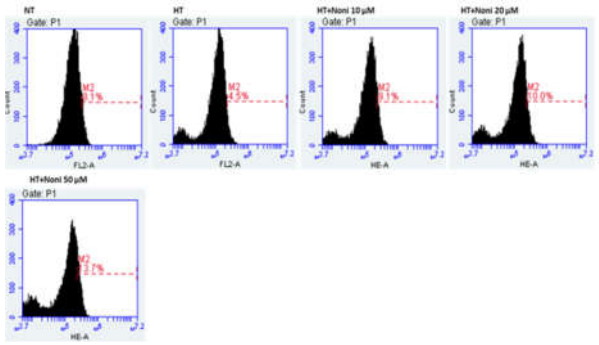

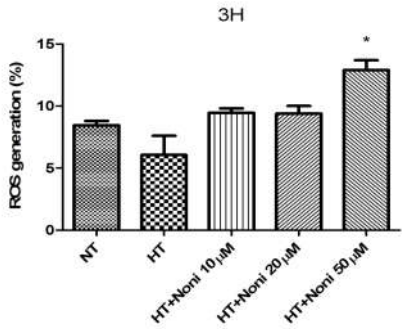

Supplement Fig. 3B

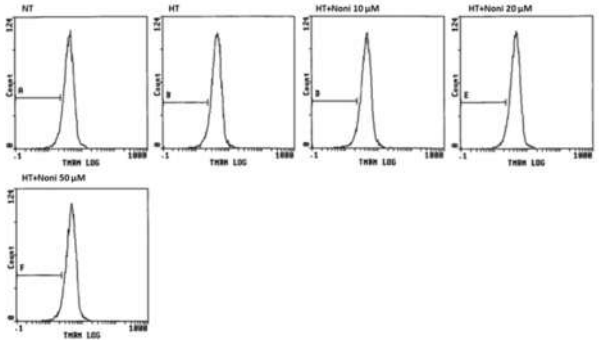

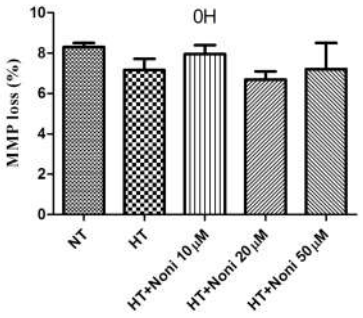

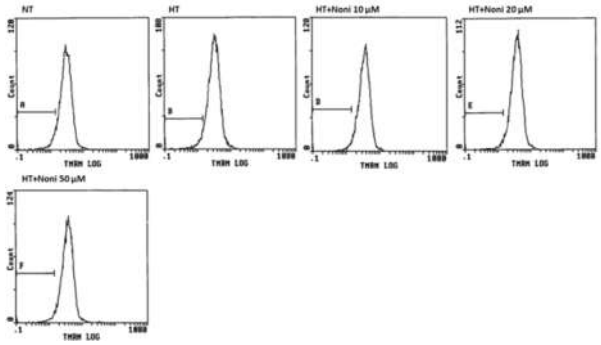

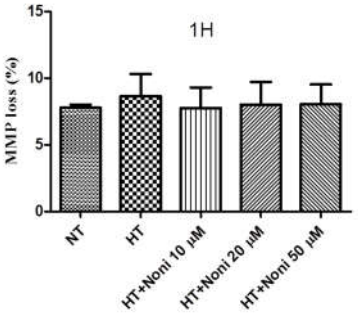

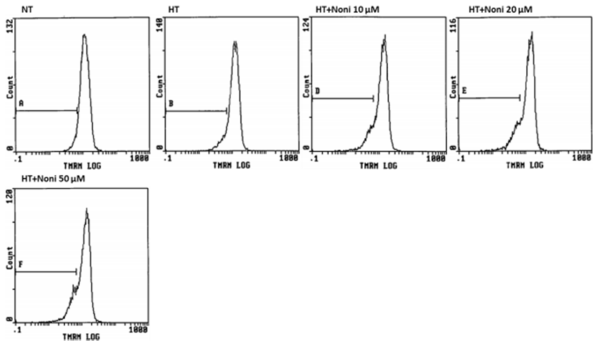

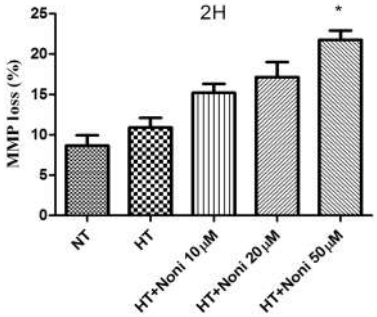

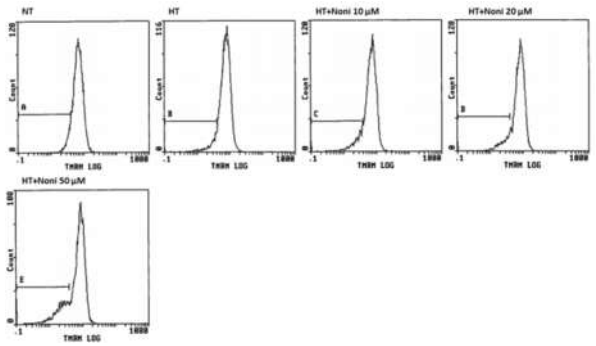

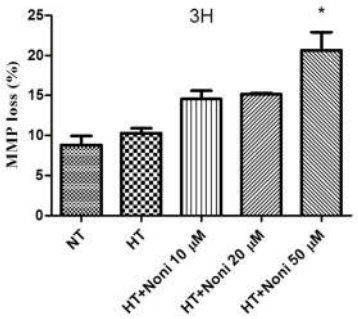

Supplement Fig. 3C

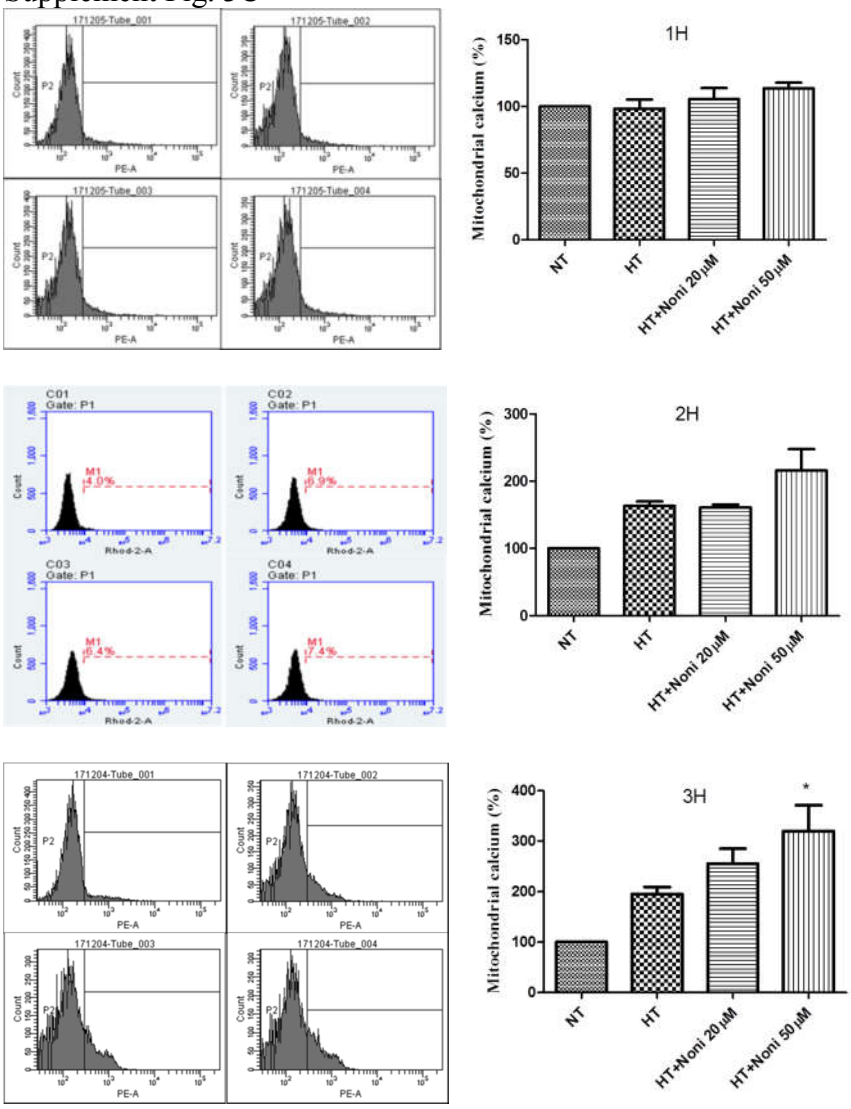

Supplemental Figure 3: Time course studies of nonivamide combined hyperthermia treatment effects on ROS generation and mitochondrial dysfunction.

Time course of the fraction of cells with increased superoxide production, estimated by flow cytometry in cells stained with DHE (A). Time course of the fraction of cells with increased MMP loss, estimated by flow cytometry in cells stained with TMRM (B). Time course of the fraction of cells with increased mitochondrial calcium loading, estimated by flow cytometry in cells stained with Rhod-2, AM (C). Statistical analysis was performed by one-way ANOVA (Dunnett's test), in which *$p < 0.05$ versus the hyperthermia group.

Supplement Fig. 4A

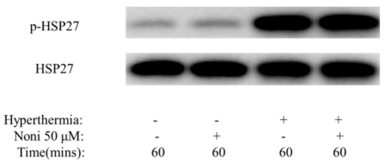

Supplement Fig. 4B

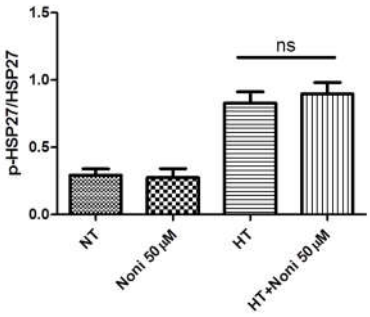

Supplement Fig. 4C

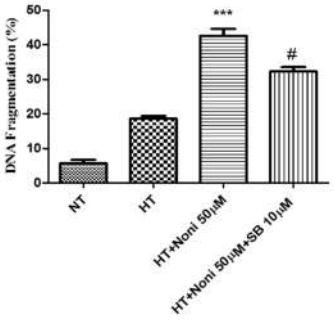

Supplement Fig. 4D

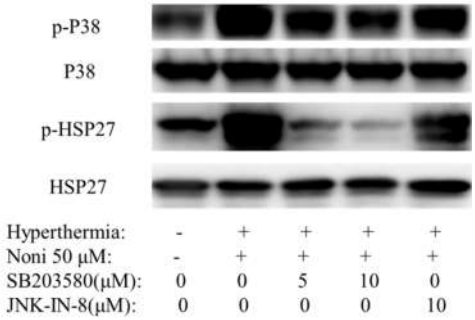

Supplement Fig. 4E

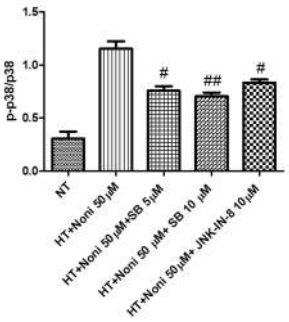

Supplement Fig. 4 F

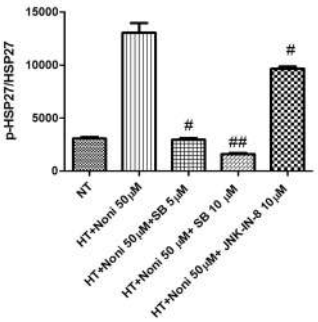

Supplement Fig. 4G

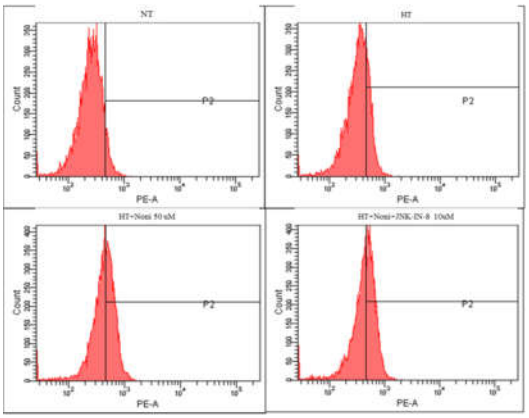

Supplement Fig. 4H

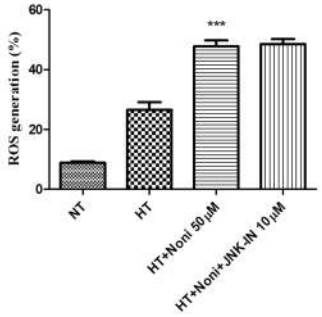

Supplement Fig. 4I

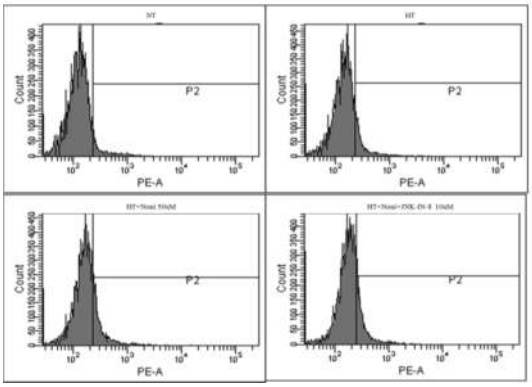

Supplement Fig. 4J

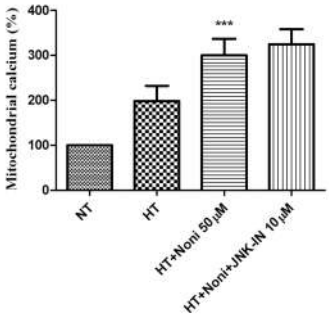

Supplement Fig. 4K

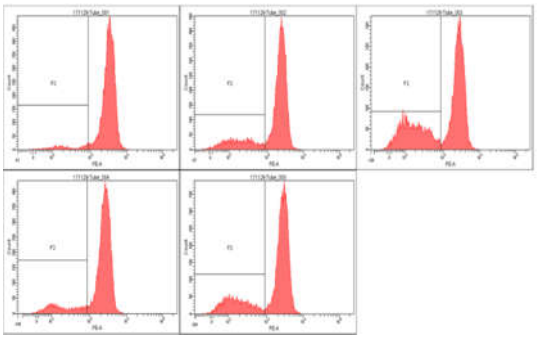

Supplement Fig. 4L

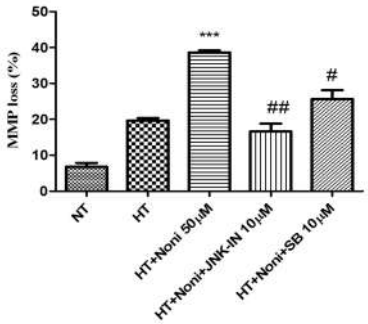

Supplemental Figure 4: JNK inhibitor VIII and SB203580 each partially rescued nonivamide combined hyperthermia treatment-induced apoptosis.

U937 cells were pre-incubated with SB203580 or JNK inhibitor VIII for 30 min, then treated with hyperthermia with nonivamide. Expressions of phosphorylated and total forms of HSP27 were analyzed by western blot (A). Average values of the ratio of phosphorylated to total proteins were quantified in each group (B). DNA fragmentation rate was determined by DNA fragmentation assay (C). Expressions of phosphorylated forms of p38 and HSP27 were analyzed by western blot (D). Average values of the ratio of phosphorylated to total proteins were quantified in each group (E, F). ROS generation was estimated by flow cytometry with DHE staining (G, H). Mitochondrial calcium loading was estimated by flow cytometry with Rhod-2, AM staining (I, J). MMP loss was estimated by flow cytometry in cells stained with TMRM (K, L). Representative data are shown from three separate experiments. The data are expressed as mean ± SEM from three independent experiments. Statistical analysis was performed by one-way ANOVA (Dunnett's test), in which ***$p < 0.01$ versus the hyperthermia group, and # $p < 0.05$ and ##$p< 0.01$ pre-treatment with the inhibitor group versus the nonivamide 50 μM combined group, ns=non-significant.

Supplement Fig. 5A

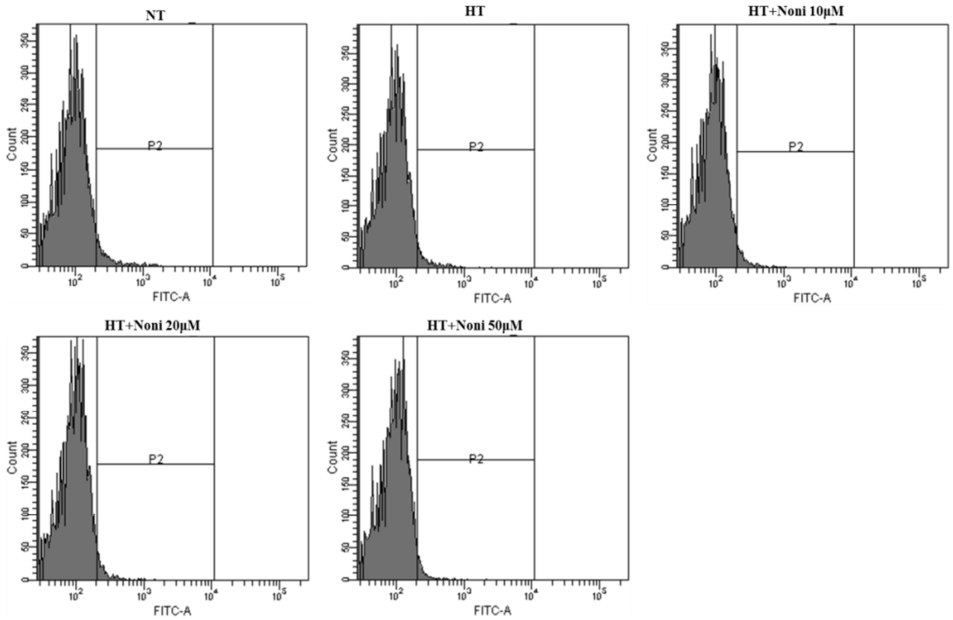

Supplement Fig. 5B

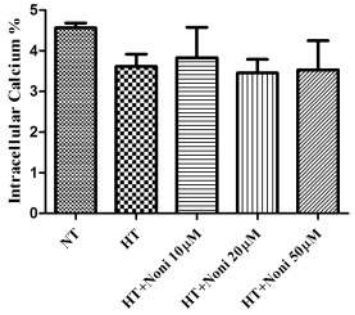

Supplemental Figure 5: Combined treatment of nonivamide with hyperthermia did not increase intracellular calcium.

Exposure of U937 cells to individual or combined treatment not disrupt the intracellular calcium concentration, which was detected by flow cytometry with Fluo-3 staining. Data are presented as mean ± SD.

Supplement Fig. 6A

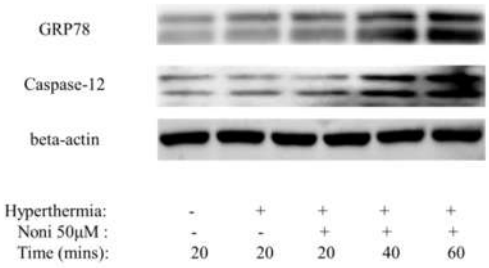

Supplement Fig. 6B

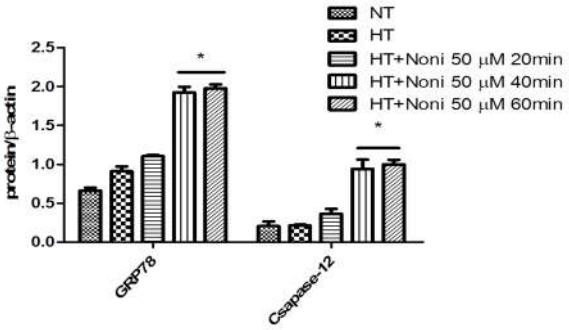

Supplement Fig. 6C

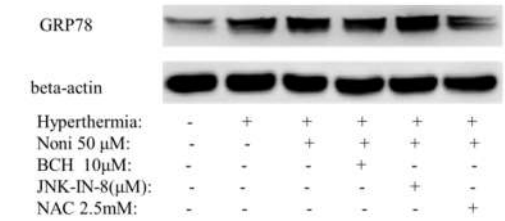

Supplement Fig. 6D

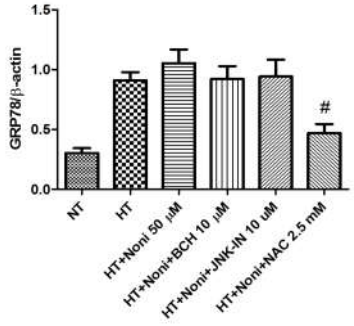

Supplemental Figure 6: Combined treatment of nonivamide with hyperthermia induced ER stress in U937 cells.

U937 cells were exposed to individual and combined treatment and the expression of GRP78 and caspase-12 was analyzed by western blot (A, C). Relative protein levels, versus control, were quantified and standardized to β-actin (B, D). Representative data are shown from three separate experiments. Statistical analysis was performed by one-way ANOVA (Dunnett's test), in which *$p < 0.05$ versus the hyperthermia group, and # $p < 0.05$ pre-treatment with the inhibitor group versus the nonivamide 50 μM combined group.

Chapter 4

Discussion

In this study, I found that nonivamide significantly enhanced hyperthermia-induced apoptosis in U937 cells. Combined nonivamide plus hyperthermia treatment increased ROS generation, JNK and p38 activation, and mitochondrial calcium loading, in addition to changing the ratio between anti- and pro-apoptotic proteins, which may contribute to disruption of mitochondrial transmembrane permeability. Further, caspase-3 was activated by both cytochrome c and phospho-PKCδ catalytic fragments. These pathways may serve as the underlying mechanisms for nonivamide enhancement of hyperthermia-induced apoptosis (Fig. 7).

Hyperthermia therapy exerts various effects, such as killing cancer cells directly; altering blood flow, oxygen, nutrient, pH, and other microenvironments; altering heat shock protein expression, cell cycle regulation, and immune response; and improving the apoptotic cascade, with or without other treatments [7]. Since the 1980s, hyperthermia has been used as an adjunct to clinical practice in various cancers. However, its application initially was restricted, possibly due to equipment limitations. Fortunately, improved technology and advancements in skill and experience have led to a reduction in the adverse effects that were originally present in hyperthermia treatment. With the accumulated experience and advanced technology available for heat delivery, many randomized phase II and III clinical trials have begun to demonstrate that hyperthermia combined with chemotherapy can be beneficial in the treatment of cancer [3,7], especially in palliative care regimens.

Heat shock proteins (HSPs) are a family of proteins that are generated by cells in response to stressful conditions. HSPs are classified based on their molecular weight: HSP27, HSP40, HSP60, HSP70, HSP90, and large HSPs [34]. Many members of this family perform chaperone functions to maintain natural structures, or to help refold

proteins following exposure to heat shock, UV light, anoxia, hypoxia, heavy metals, or drugs, as well as in cases of wound healing and/or tissue remodeling [34]. Previous studies have revealed that HSP27 inhibits apoptosis through the following mechanisms: maintenance of mitochondrial redox status and stability; modulation of apoptosis signal-regulating kinases and the AKT pathway; inhibition of cytochrome c activation caspase and inhibition of mitochondrial release endogenous proteins, which induce apoptosis [35]. HSP27 is overexpressed in pediatric acute myeloid leukemia; thus, it can be used as a biomarker in cancer diagnosis [36]. Therefore, I measured HSP27 expression in our experiments, and found that neither hyperthermia alone, nor hyperthermia combined with nonivamide treatment, led to increased HSP27 expression (Supplemental Fig. 4A). In response to stress, HSP27 is phosphorylated at Ser-15, Ser-78, and Ser-82 by mitogen-activated protein kinase-activated protein kinases (MAPKAPK) 2 and 3, following activation of the p38 MAPK pathway. In our data, hyperthermia clearly caused increased p-HSP27 expression. However, nonivamide alone did not increase p-HSP27 expression (Supplemental Fig. 4B). Hyperthermia combined with nonivamide treatment did not exert a synergistic effect in increasing p-HSP27 expression; importantly, the hyperthermia-induced upregulation of expression was significantly reduced by a p38 inhibitor (SB203580) (Supplemental Fig. 4D). Therefore, it appears that HSP27 does not participate in hyperthermia combined with nonivamide-induced apoptosis.

The Scoville scale is a method for measuring capsaicinoid concentration. Capsaicin, as the “gold standard” for hotness, is rated with 16 million Scoville heat units (SHU) [37]. Many reports have indicated that capsaicin can be a potent cancer chemo-preventive compound [37]. Unfortunately, several epidemiological studies have shown that uptake of capsaicin could increase the risk of gallbladder or gastric cancer [37]. Therefore, the European Union has not yet approved the use of capsaicin as a food additive [38].

Nonivamide, with 9.2 million SHU, is found in natural chili peppers. It has a less spicy effect and is more acceptable than capsaicin, and is permitted as a food additive in the European Union (FEMA 2787 and FL No. 16.006 http://data.europa.eu/eli/reg_impl/2012/872/oj). Moreover, nonivamide exhibits anti-inflammatory effects, and can cause increased serotonin in peripheral cells [14,39]. In general, cancer patients suffer from a variety of painful stimuli. Nonivamide exerts analgesic action, which increases the anti-nociceptive and anti-inflammatory neuropeptide somatostatin in patients with chronic low back pain [40]. Thus far, few reports have discussed the application of nonivamide in cancer therapy. Therefore, I undertook this study of nonivamide to determine its anti-cancer effects and the associated molecular mechanisms. Combining previous studies [41] and our current data, nonivamide and capsaicin appear to have a similar effect in suppressing cell proliferation and inducing apoptosis; capsaicin 50 μM combined with hyperthermia did not induce a significantly different level of U937 cell death, compared with nonivamide 50 μM plus hyperthermia (Supplemental Fig. 1D). Previously, nonivamide demonstrated anti-inflammatory effects in U937 cells; BCH abrogated this effect via the transient receptor protein (TRP) channel [14]. Our data also indicated that BCH partially rescued apoptosis that was induced by nonivamide combined treatment (Fig. 6A). In contrast, BCH was incapable of reducing ROS generation (data not shown), mitochondrial calcium loading (Fig. 3D), or p-JNK expression (Fig. 6C), all of which were increased following nonivamide combined treatment. I found that BCH inhibited nonivamide upregulated heme oxygenase-1 (HO-1) expression (data not shown), perhaps through reduced augmentation of apoptosis via the HO-1 pathway. Thus, the TRPV1 channel was not involved in nonivamide-enhanced hyperthermia-induced apoptosis. TRPV1 antagonists, in addition to blocking the TRPV1 channel, exhibit different biological activities; for

example, AMG517 causes hyperthermia [42], AMG9810 promotes mouse skin tumorigenesis [43], and capsazepine induces colorectal cancer apoptosis [44]. It was previously unclear whether capsaicin analogues could induce apoptosis via TRPV1-dependent pathways [45,46]. Taken together, our results (i.e., TRPV1 antagonist capsazepine enhanced hyperthermia-induced apoptosis) support this hypothesis. In the future, more detailed studies are required to further clarify this point.

BCH is selective TRPV1 antagonist. This antagonist is able to inhibit capsaicin-induced TRPV1 activation. No inhibitory effect of BCH was measured on TRPA1, TRPV3 and TRPM8 in the oocyte model [47]. So far, some paper reported BCH could decrease TRPV1 activation. The antagonist affinity and exact mechanism is unknown, which needs further study.

ROS generation is considered a natural byproduct of the normal metabolism of oxygen. Upregulation of ROS generation plays important roles in cell signaling and regulating apoptosis, especially in enhancing mitochondrial calcium uptake [7]. Hyperthermia increases ROS generation, and capsaicin can enhance tumor cell apoptosis via ROS generation [15,18]. In addition, a previous study revealed that glyceryl nonivamide upregulated ROS generation in SH-SY5Y cells [48]. Mitochondrial calcium uniporter (MCU) has been identified as a mitochondrial calcium uptake channel; MCU dysfunction, caused by ROS generation, leads to calcium overload and disruption of MMP. Furthermore, hyperthermia has been shown to induce cell apoptosis via MCU-mediated mitochondrial calcium overload [49,50]. Our findings suggest that nonivamide enhances hyperthermia-induced ROS generation, and that production of ROS can be decreased by combined treatment with the ROS scavenger NAC (Fig. 2B). In addition, NAC abolished increased mitochondrial calcium loading (Fig. 3D) and induction of

apoptosis (Fig. 6B) that were caused by nonivamide combined treatment. Therefore, MCU may be a target for mediation of U937 cell apoptosis.

ER stress possibly contributed to nonivamide enhancement of hyperthermia-induced apoptosis, as demonstrated by GRP78 and caspase-12 induction (Supplement Fig. 6). GRP78, also known as binding immunoglobulin protein (BiP), was a target of the ER stress response or unfolded protein response (UPR) [51]. As previous studies have indicated, ER stress induces apoptosis by upregulating JNK and caspase-12 expression, while downregulating Bcl-2 expression [52]. ER stress is sufficient to alter redox homeostasis; subsequently, the altered redox homeostasis induces ROS generation in the ER and mitochondria [52]. Moreover, calcium signaling is involved in ROS generation and ER stress [8]. In our study, it appears that calcium, ROS generation, and ER stress combined to regulate cell apoptosis.

When extracted from fresh peppers, the range of nonivamide concentration is 0.42%–7.2% [53]. For conceptual analysis, I assumed extraction of nonivamide 1% from fresh peppers. An adult patient contains 4 L blood volume; thus, to reach a concentration of 50 μM (59 mg/4 L), this patient would need to consume 5.9 g green bell peppers [53]. Although it is physically possible to consume this quantity of fresh pepper, the human gastrointestinal tract cannot absorb more than 0.15 mg nonivamide [14,39]. Furthermore, excessive intake of hot peppers might be increase the risk of gallbladder or gastric cancer. Notably, subcutaneous injection of nonivamide in rats decreased body temperature and caused vasodilatation [54]. Thus, subcutaneous, intraperitoneal, or intravenous injection of nonivamide may serve as optimal treatment modalities. To better understand the potential of nonivamide in cancer therapy, further *in vivo* research is required.

Chapter 5

Conclusion

I have demonstrated that treatment with nonivamide, prior to hyperthermia, boosts apoptosis in U937 cells. Enhanced ROS generation may be a possible mechanism of the enhanced apoptotic effect that is observed with this combined treatment. Furthermore, nonivamide enhanced apoptotic cell death when combined with hyperthermia, via the MAPK pathway and mitochondrial dysfunction. Enhancing hyperthermia treatment using nonivamide represents an advancement in cancer therapeutics.

References

[1] R.D. Issels, Hyperthermia adds to chemotherapy, Eur. J. Cancer. 44 (2008) 2546–2554. doi:10.1016/j.ejca.2008.07.038.

[2] J. van der Zee, Heating the patient: a promising approach?, Ann. Oncol. Off. J. Eur. Soc. Med. Oncol. 13 (2002) 1173–84. doi:10.1093/annonc/mdf280.

[3] P. Wust, B. Hildebrandt, G. Sreenivasa, B. Rau, J. Gellermann, H. Riess, R. Felix, P. Schlag, Hyperthermia in combined treatment of cancer, Lancet Oncol. 3 (2002) 487–497. doi:10.1016/S1470-2045(02)00818-5.

[4] C. Quintana, J. Cabrera, J. Perdomo, F. Estévez, J.F. Loro, R.J. Reiter, J. Quintana, Melatonin enhances hyperthermia-induced apoptotic cell death in human leukemia cells, J. Pineal Res. 61 (2016) 381–395. doi:10.1111/jpi.12356.

[5] R.S. Wong, Apoptosis in cancer: from pathogenesis to treatment, J. Exp. Clin. Cancer Res. 30 (2011) 87. doi:10.1186/1756-9966-30-87.

[6] M. Hassan, H. Watari, A. AbuAlmaaty, Y. Ohba, N. Sakuragi, Apoptosis and Molecular Targeting Therapy in Cancer, Biomed Res. Int. 2014 (2014) 1–23. doi:10.1155/2014/150845.

[7] T. Mantso, G. Goussetis, R. Franco, S. Botaitis, A. Pappa, M. Panayiotidis, Effects of hyperthermia as a mitigation strategy in DNA

damage-based cancer therapies., Semin. Cancer Biol. 37–38 (2016) 96–105. doi:10.1016/j.semcancer.2016.03.004.

[8] A. Görlach, K. Bertram, S. Hudecova, O. Krizanova, Calcium and ROS: A mutual interplay, Redox Biol. 6 (2015) 260–271. doi:10.1016/j.redox.2015.08.010.

[9] Z.T. Gu, L. Li, F. Wu, P. Zhao, H. Yang, Y.S. Liu, Y. Geng, M. Zhao, L. Su, Heat stress induced apoptosis is triggered by transcription-independent p53, Ca(2+) dyshomeostasis and the subsequent Bax mitochondrial translocation., Sci. Rep. 5 (2015) 11497. doi:10.1038/srep11497.

[10] M.S. Ricci, W. Zong, L. Objectives, Chemotherapeutic Approaches for Targeting Cell Death Pathways, Oncologist. (2006). doi:10.1634/theoncologist.11-4-342.

[11] B. Rohm, A.-K. Holik, M.M. Somoza, M. Pignitter, M. Zaunschirm, J.P. Ley, G.E. Krammer, V. Somoza, Nonivamide, a capsaicin analog, increases dopamine and serotonin release in SH-SY5Y cells via a TRPV1-independent pathway., Mol. Nutr. Food Res. 57 (2013) 2008–18. doi:10.1002/mnfr.201200846.

[12] B. Rohm, A.-K. Holik, N. Kretschy, M.M. Somoza, J.P. Ley, S. Widder, G.E. Krammer, D. Marko, V. Somoza, Nonivamide enhances miRNA let-7d expression and decreases adipogenesis PPARγ

expression in 3T3-L1 cells., J. Cell. Biochem. 116 (2015) 1153–63. doi:10.1002/jcb.25052.

[13] B. Rohm, A. Riedel, J.P. Ley, S. Widder, G.E. Krammer, V. Somoza, Capsaicin, nonivamide and trans-pellitorine decrease free fatty acid uptake without TRPV1 activation and increase acetyl-coenzyme A synthetase activity in Caco-2 cells., Food Funct. 6 (2015) 173–85. doi:10.1039/c4fo00435c.

[14] J. Walker, J.P. Ley, J. Schwerzler, B. Lieder, L. Beltran, P.M. Ziemba, H. Hatt, J. Hans, S. Widder, G.E. Krammer, V. Somoza, Nonivamide, a capsaicin analogue, exhibits anti-inflammatory properties in peripheral blood mononuclear cells and U-937 macrophages., Mol. Nutr. Food Res. 61 (2017) 1600474. doi:10.1002/mnfr.201600474.

[15] A.M. Chapa-Oliver, L. Mejía-Teniente, Capsaicin: From Plants to a Cancer-Suppressing Agent., Molecules. 21 (2016) 931. doi:10.3390/molecules21080931.

[16] N. Rivlin, R. Brosh, M. Oren, V. Rotter, Mutations in the p53 Tumor Suppressor Gene: Important Milestones at the Various Steps of Tumorigenesis., Genes Cancer. 2 (2011) 466–74. doi:10.1177/1947601911408889.

[17] A. Garufi, G. Pistritto, M. Cirone, G. D'Orazi, Reactivation of mutant p53 by capsaicin, the major constituent of peppers., J. Exp. Clin. Cancer Res. 35 (2016) 136. doi:10.1186/s13046-016-0417-9.

[18] K. Ito, T. Nakazato, K. Yamato, Y. Miyakawa, T. Yamada, N. Hozumi, K. Segawa, Y. Ikeda, M. Kizaki, Induction of apoptosis in leukemic cells by homovanillic acid derivative, capsaicin, through oxidative stress: implication of phosphorylation of p53 at Ser-15 residue by reactive oxygen species., Cancer Res. 64 (2004) 1071–8. doi:10.1158/0008-5472.CAN-03-1670.

[19] L. Sun, Z.-G. Cui, S.A. Zakki, Q.-W. Feng, M.-L. Li, H. Inadera, Mechanistic study of nonivamide enhancement of hyperthermia-induced apoptosis in U937 cells., Free Radic. Biol. Med. 120 (2018) 147–159. doi:10.1016/j.freeradbiomed.2018.03.017.

[20] K. Hertveldt, J. Philippé, H. Thierens, M. Cornelissen, A. Vral, L. De Ridder, Flow cytometry as a quantitative and sensitive method to evaluate low dose radiation induced apoptosis in vitro in human peripheral blood lymphocytes., Int. J. Radiat. Biol. 71 (1997) 429–33. doi:10.1080/095530097144049.

[21] C. Riccardi, I. Nicoletti, Analysis of apoptosis by propidium iodide staining and flow cytometry., Nat. Protoc. 1 (2006) 1458–61. doi:10.1038/nprot.2006.238.

[22] K.S. Sellins, J.J. Cohen, Gene induction by gamma-irradiation leads to DNA fragmentation in lymphocytes., J. Immunol. 139 (1987) 3199–206.

[23] M. Li, T. Kondo, Q.-L. Zhao, F.-J. Li, K. Tanabe, Y. Arai, Z.-C. Zhou, M. Kasuya, Apoptosis Induced by Cadmium in Human Lymphoma U937 Cells through Ca2+-calpain and Caspase-Mitochondria-dependent Pathways, J. Biol. Chem. 275 (2000) 39702–39709. doi:10.1074/jbc.M007369200.

[24] Z. Cui, J. Piao, M.U.R. Rehman, R. Ogawa, P. Li, Q. Zhao, T. Kondo, H. Inadera, Molecular mechanisms of hyperthermia-induced apoptosis enhanced by withaferin A, Eur. J. Pharmacol. 723 (2014) 99–107. doi:10.1016/j.ejphar.2013.11.031.

[25] Z.-G. Cui, T. Kondo, H. Matsumoto, Enhancement of apoptosis by nitric oxide released from α-phenyl-tert-butyl nitrone under hyperthermic conditions, J. Cell. Physiol. 206 (2006) 468–476. doi:10.1002/jcp.20482.

[26] B. Joe, B.R. Lokesh, Role of capsaicin, curcumin and dietary n-3 fatty acids in lowering the generation of reactive oxygen species in rat peritoneal macrophages., Biochim. Biophys. Acta. 1224 (1994) 255–63. doi:10.1016/0167-4889(94)90198-8.

[27] F.K. Storm, W.H. Harrison, R.S. Elliott, D.L. Morton, Normal tissue and solid tumor effects of hyperthermia in animal models and clinical trials., Cancer Res. 39 (1979) 2245–51. http://www.ncbi.nlm.nih.gov/pubmed/445424.

[28] Z.-G. Cui, T. Kondo, L.B. Feril, Jr., K. Waki, O. Inanami, M. Kuwabara, Effects of antioxidants on X-ray- or hyperthermia-induced apoptosis in human lymphoma U937 cells, Apoptosis. 9 (2004) 757–763. doi:10.1023/B:APPT.0000045782.56480.6b.

[29] D. De Stefani, R. Rizzuto, T. Pozzan, Enjoy the Trip: Calcium in Mitochondria Back and Forth, Annu. Rev. Biochem. 85 (2016) 161–192. doi:10.1146/annurev-biochem-060614-034216.

[30] M. Zhao, L. Xia, G.-Q. Chen, Protein kinase cδ in apoptosis: a brief overview., Arch. Immunol. Ther. Exp. (Warsz). 60 (2012) 361–72. doi:10.1007/s00005-012-0188-8.

[31] B.-C. Jang, K.-J. Lim, J.-H. Paik, J.-W. Cho, W.-K. Baek, M.-H. Suh, J.-B. Park, T.K. Kwon, J.-W. Park, S.-P. Kim, D.-H. Shin, D. Song, J.-H. Bae, K.-C. Mun, S.-I. Suh, Tetrandrine-induced apoptosis is mediated by activation of caspases and PKC-δ in U937 cells, Biochem. Pharmacol. 67 (2004) 1819–1829. doi:10.1016/j.bcp.2004.01.018.

[32] Z. Cui, J. Piao, T. Kondo, R. Ogawa, K. Tsuneyama, Q. Zhao, L.B. Feril, H. Inadera, Molecular mechanisms of hyperthermia-induced apoptosis enhanced by docosahexaenoic acid: Implication for cancer therapy, Chem. Biol. Interact. 215 (2014) 46–53. doi:10.1016/j.cbi.2014.03.005.

[33] M. Rahmani, M.M. Aust, E. Attkisson, D.C. Williams, A. Ferreira-Gonzalez, S. Grant, Dual inhibition of Bcl-2 and Bcl-xL strikingly

enhances PI3K inhibition-induced apoptosis in human myeloid leukemia cells through a GSK3- and Bim-dependent mechanism., Cancer Res. 73 (2013) 1340–51. doi:10.1158/0008-5472.CAN-12-1365.

[34] J. Wu, T. Liu, Z. Rios, Q. Mei, X. Lin, S. Cao, Heat Shock Proteins and Cancer., Trends Pharmacol. Sci. 38 (2017) 226–256. doi:10.1016/j.tips.2016.11.009.

[35] E.E. Benarroch, Heat shock proteins: multiple neuroprotective functions and implications for neurologic disease., Neurology. 76 (2011) 660–7. doi:10.1212/WNL.0b013e31820c3119.

[36] E. V. Mymrikov, A.S. Seit-Nebi, N.B. Gusev, Large potentials of small heat shock proteins., Physiol. Rev. 91 (2011) 1123–59. doi:10.1152/physrev.00023.2010.

[37] A.M. Bode, Z. Dong, The two faces of capsaicin., Cancer Res. 71 (2011) 2809–14. doi:10.1158/0008-5472.CAN-10-3756.

[38] EFSA, Regulation (EC) No 1334/2008 of the European Parliament and of the Council of 16 December 2008 on flavourings and certain food ingredients with flavouring properties for use in and on foods and amending Council Regulation (EEC) No 1601/91, Regul, 2008.

[39] C.M. Hochkogler, B. Lieder, P. Rust, D. Berry, S.M. Meier, M. Pignitter, A. Riva, A. Leitinger, A. Bruk, S. Wagner, J. Hans, S. Widder, J.P. Ley, G.E. Krammer, V. Somoza, A 12-week intervention

with nonivamide, a TRPV1 agonist, prevents a dietary-induced body fat gain and increases peripheral serotonin in moderately overweight subjects., Mol. Nutr. Food Res. 61 (2017) 1600731. doi:10.1002/mnfr.201600731.

[40] K. Horváth, M. Boros, T. Bagoly, V. Sándor, F. Kilár, A. Kemény, Z. Helyes, J. Szolcsányi, E. Pintér, Analgesic topical capsaicinoid therapy increases somatostatin-like immunoreactivity in the human plasma., Neuropeptides. 48 (2014) 371–8. doi:10.1016/j.npep.2014.10.001.

[41] J.-L. Piao, Y.-J. Jin, M.-L. Li, S.A. Zakki, L. Sun, Q.-W. Feng, D. Zhou, T. Kondo, Z.-G. Cui, H. Inadera, Excessive Oxidative Stress in the Synergistic Effects of Shikonin on the Hyperthermia-Induced Apoptosis., Curr. Mol. Med. 18 (2018) 322–334. doi:10.2174/1566524018666181024161704.

[42] A. Garami, Y.P. Shimansky, E. Pakai, D.L. Oliveira, N.R. Gavva, A.A. Romanovsky, Contributions of different modes of TRPV1 activation to TRPV1 antagonist-induced hyperthermia., J. Neurosci. 30 (2010) 1435–40. doi:10.1523/JNEUROSCI.5150-09.2010.

[43] S. Li, A.M. Bode, F. Zhu, K. Liu, J. Zhang, M.O. Kim, K. Reddy, T. Zykova, W. Ma, A.L. Carper, A.K. Langfald, Z. Dong, TRPV1-antagonist AMG9810 promotes mouse skin tumorigenesis through

EGFR/Akt signaling., Carcinogenesis. 32 (2011) 779–85. doi:10.1093/carcin/bgr037.

[44] B. Sung, S. Prasad, J. Ravindran, V.R. Yadav, B.B. Aggarwal, Capsazepine, a TRPV1 antagonist, sensitizes colorectal cancer cells to apoptosis by TRAIL through ROS-JNK-CHOP-mediated upregulation of death receptors., Free Radic. Biol. Med. 53 (2012) 1977–87. doi:10.1016/j.freeradbiomed.2012.08.012.

[45] S.A. Omari, M.J. Adams, D.A. Kunde, D.P. Geraghty, Capsaicin-Induced Death of Human Haematological Malignant Cell Lines Is Independent of TRPV1 Activation., Pharmacology. 98 (2016) 79–86. doi:10.1159/000445437.

[46] M. Maccarrone, T. Lorenzon, M. Bari, G. Melino, A. Finazzi-Agro, Anandamide induces apoptosis in human cells via vanilloid receptors. Evidence for a protective role of cannabinoid receptors., J. Biol. Chem. 275 (2000) 31938–45. doi:10.1074/jbc.M005722200.

[47] T. Kueper, M. Krohn, L.O. Haustedt, H. Hatt, G. Schmaus, G. Vielhaber, Inhibition of TRPV1 for the treatment of sensitive skin., Exp. Dermatol. 19 (2010) 980–6. doi:10.1111/j.1600-0625.2010.01122.x.

[48] Y.-C. Lin, H.-W. Uang, R.-J. Lin, I.-J. Chen, Y.-C. Lo, Neuroprotective effects of glyceryl nonivamide against microglia-like cells and 6-hydroxydopamine-induced neurotoxicity in SH-SY5Y

human dopaminergic neuroblastoma cells., J. Pharmacol. Exp. Ther. 323 (2007) 877–87. doi:10.1124/jpet.107.125955.

[49] Z. Dong, C. Zhang, Y. Chen, Y. Chen, Z. Yuan, Y. Peng, T. Cao, Astragaloside-IV Protects Against Heat-induced Apoptosis by Inhibiting Excessive Activation of Mitochondrial Ca2+ Uniporter., Cell. Physiol. Biochem. 42 (2017) 480–494. doi:10.1159/000477595.

[50] L. Li, H. Tan, Z. Gu, Z. Liu, Y. Geng, Y. Liu, H. Tong, Y. Tang, J. Qiu, L. Su, Heat stress induces apoptosis through a Ca^{2+}-mediated mitochondrial apoptotic pathway in human umbilical vein endothelial cells., PLoS One. 9 (2014) e111083. doi:10.1371/journal.pone.0111083.

[51] M. Høyer-Hansen, M. Jäättelä, Connecting endoplasmic reticulum stress to autophagy by unfolded protein response and calcium., Cell Death Differ. 14 (2007) 1576–82. doi:10.1038/sj.cdd.4402200.

[52] L. Zhou, L. Jiang, M. Xu, Q. Liu, N. Gao, P. Li, E. Liu, Miltirone exhibits antileukemic activity by ROS-mediated endoplasmic reticulum stress and mitochondrial dysfunction pathways., Sci. Rep. 6 (2016) 20585. doi:10.1038/srep20585.

[53] C. a Reilly, D.J. Crouch, G.S. Yost, Quantitative analysis of capsaicinoids in fresh peppers, oleoresin capsicum and pepper spray products., J. Forensic Sci. 46 (2001) 502–9. http://www.ncbi.nlm.nih.gov/pubmed/11372985.

[54] EMEA/MRL/467/98-FINAL Committee for veterinary medicinal products nonivamide summary report, 1998. http://www.ema.europa.eu/docs/en_GB/document_library/Maximum_Residue_Limits_-_Report/2009/11/WC500015186.pdf.

Acknowledgements

My supervisor Hidekuni Inadera:

Thank you for your patience and endless support. You have given me the opportunity to work independently. At the same time, your door has always been open, and you have been there to support, discuss and help me progress, at any time! I appreciate your stability and warm heart.

To all past and present members of the lab:

I would like to express my sincere appreciation and praises to Dr. Zheng-Guo Cui, for his countless efforts, kind supervision and friendly companionship which boosted me up to strive for excellence. Ms. Nozomi Kawaguchi, who provided her kind assistance in completing basic documentation. It is my pleasure to record my heartfelt applause to all my laboratory colleagues, especially to Dr. Shahbaz Ahmad Zakki, Dr. Yu-Jie Jin, Dr. Meng-Ling Li, Dr. Qian-Wen Feng. Dr. Yu-Lin Li with whom I spend important time of my life in Toyama with cheerful gatherings, enthusiastic research activities and assisting each others to cope with hardships of life.

Sun Lu